CHRONIC KIDNEY DISEASE

Calprotectin is a contributor to and potential therapeutic target for vascular calcification in chronic kidney disease

Ana Amaya-Garrido[1,2], Manon Brunet[1,2], Bénédicte Buffin-Meyer[1,2], Alexis Piedrafita[1,2,3], Lucile Grzesiak[1,2], Ezechiel Agbegbo[1,2], Arnaud Del Bello[3], Inés Ferrandiz[3], Serban Ardeleanu[4], Marcelino Bermudez-Lopez[5], Camille Fedou[1,2]†, Mylène Camus[6], Odile Burlet-Schiltz[6], Jean Massines[1,2], Marie Buléon[1,2], Guylène Feuillet[1,2], Melinda Alves[1,2], Eric Neau[1,2], Audrey Casemayou[1,2,3], Benjamin Breuil[1,2], Jean-Sébastien Saulnier-Blache[1,2], Colette Denis[1,2], Jakob Voelkl[7,8,9], Griet Glorieux[10], Sam Hobson[11], Samsul Arefin[11], Awahan Rahman[11], Karolina Kublickiene[11], Peter Stenvinkel[11], Jean-Loup Bascands[12], Stanislas Faguer[1,2,3], José M. Valdivielso[5], Joost P. Schanstra[1,2]*, Julie Klein[1,2]*

Vascular calcification is an important risk factor for cardiovascular (CV) mortality in patients with chronic kidney disease (CKD). It is also a complex process involving osteochondrogenic differentiation of vascular smooth muscle cells (VSMCs) and abnormal deposition of minerals in the vascular wall. In an observational, multicenter European study, including 112 patients with CKD from Spain and 171 patients on dialysis from France, we used serum proteome analysis and further validation by ELISA to identify calprotectin, a circulating damage-associated molecular pattern protein, as being independently associated with CV outcome and mortality. This was confirmed in an additional cohort of 170 patients with CKD from Sweden, where increased serum calprotectin concentrations correlated with increased vascular calcification. In primary human VSMCs and mouse aortic rings, calprotectin exacerbated calcification. Treatment with paquinimod, a calprotectin inhibitor, as well as pharmacological inhibition of the receptor for advanced glycation end products and Toll-like receptor 4 inhibited the procalcifying effect of calprotectin. Paquinimod also ameliorated calcification induced by the sera of uremic patients in primary human VSMCs. Treatment with paquinimod prevented vascular calcification in mice with chronic renal failure induced by subtotal nephrectomy and in aged apolipoprotein E–deficient mice as well. These observations identified calprotectin as a key contributor of vascular calcification, and increased circulating calprotectin was strongly and independently associated with calcification, CV outcome, and mortality in patients with CKD. Inhibition of calprotectin might therefore be a promising strategy to prevent vascular calcification in patients with CKD.

INTRODUCTION

Chronic kidney disease (CKD) is a major cause of mortality and a leading risk factor for cardiovascular (CV) complications (*1*). Compared with the general population, patients with CKD stage 3 and 4 have a two- to threefold increased risk of CV mortality, and this risk further increases up to 20-fold in patients with CKD stage 5 on dialysis (*2*). Common risk factors, such as diabetes, hypertension, smoking and dyslipidemia, and disease-specific risk factors, such as accumulation of uremic toxins, inflammation, and bone mineral disorders, contribute to the increased risk of CV complications in patients with CKD (*2*). The main CKD-associated CV complications are atherosclerosis, which is accelerated in this context but not specific of CKD, and specific CKD-related vascular calcification (*2*). Vascular calcification is closely associated with increased morbidity and mortality in patients with CKD (*3*, *4*).

After exposure to procalcific factors, including hyperphosphatemia or inflammation driven by CKD, vascular smooth muscle cells (VSMCs) present in the arterial wall switch from a contractile to an osteochondrogenic phenotype. This transdifferentiation involves the up-regulation of osteochondrogenic transcription factors, including Runt-related transcription factor 2 (*Runx2*) or Msh homeobox 2 (*Msx2*) (*5*). Furthermore, activation of the osteogenic enzyme tissue nonspecific alkaline phosphatase (*ALPL*) inactivates the calcification inhibitor pyrophosphate, allowing for the formation of

[1]Institut National de la Santé et de la Recherche Médicale (INSERM), U1297, Institute of Cardiovascular and Metabolic Disease, 31432 Toulouse, France. [2]Université Toulouse III Paul-Sabatier, 31062 Toulouse, France. [3]Département de Néphrologie et Transplantation d'organes, Hôpital Rangueil, Centre Hospitalo-Universitaire de Toulouse, 31400 Toulouse, France. [4]AURAR Saint Louis Dialysis Center, 97421 Saint Louis, La Réunion, France. [5]Vascular and Renal Translational Research Group, UDETMA, REDinREN del ISCIII, IRBLleida, 25198 Lleida, Spain. [6]Institut de Pharmacologie et Biologie Structurale, IPBS, Université de Toulouse, CNRS, UPS, 31400 Toulouse, France. [7]Institute for Physiology and Pathophysiology, Johannes Kepler University Linz, 4040 Linz, Austria. [8]DZHK (German Centre for Cardiovascular Research), Partner Site Berlin, 10785 Berlin, Germany. [9]Department of Nephrology and Medical Intensive Care, Charité-Universitätsmedizin Berlin, 10117 Berlin, Germany. [10]Nephrology Section, Department of Internal Medicine and Pediatrics, Ghent University Hospital, 9000 Gent, Belgium. [11]Division of Renal Medicine, Department of Clinical Science, Technology and Intervention, Karolinska Institutet, 14186 Stockholm, Sweden. [12]Institut National de la Santé et de la Recherche Médicale (INSERM), U1188, Diabète athérothrombose Thérapies Réunion Océan Indien (DéTROI), Université de La Réunion, 97491 Sainte Clotilde, La Réunion, France.
*Corresponding author. Email: julie.klein@inserm.fr (J.K.); joost-peter.schanstra@inserm.fr (J.P.S.)
†Present address: Ambiotis, 31400 Toulouse, France.

hydroxyapatite from calcium and phosphate (*5*). Hydroxyapatite accumulates in the vessel wall, either in the medial layer, leading to stiffness and eventually left-ventricular hypertrophy, or in the intimal layer, associated with atherosclerosis, plaque rupture, and myocardial infarction (*6*). Whereas intimal calcification is associated with atherosclerosis, medial calcification is characteristic of CKD and is up to 45-fold more prevalent than in individuals without CKD, although it is also increased in individuals with diabetes and aging (*7*).

Although the close link between vascular calcification, CV complications, and decline in kidney function is undeniable, the mechanisms of this complex interaction are still incompletely understood. Recently, considerable effort has been devoted to identifying the plethora of contributors and predictive risk factors for CV disease in patients with CKD. In particular, the comprehensive evaluation of serum and plasma proteomic profiles between healthy individuals or patients at different stages of CKD, with or without dialysis, has substantially improved the knowledge of circulating factors associated with the progression of renal dysfunction (*8*–*10*). However, in most cases, these studies were not initially designed to assess the potential association of identified factors with CV outcome and/or targeted a limited number of proteins using specific panels of candidates already known to be associated with inflammation, CKD, or CV disease. Moreover, despite intensive research efforts over the past decade, no specific treatments have been identified to prevent or slow vascular calcification (*7*, *11*), which has a considerable impact on the survival of patients with CKD. A recent randomized phase 2 study of SNF472 (hexasodium phytate), a selective inhibitor of hydroxyapatite formation, showed encouraging results in attenuating the progression of vascular calcification in hemodialysis patients (*12*). However, concerns have been raised about the potential side effects of this drug on bone formation and bone mineral density because hydroxyapatite is the major physiological mineral component of bone (*12*). For this reason, there is an urgent need to better understand the mechanisms of vascular calcification and to develop new drugs that would target pathological extra-osseous calcification.

In this study, we identified calprotectin, a circulating damage-associated molecular pattern (DAMP) protein, as a contributor to and therapeutic target for vascular calcification in patients with CKD. Using serum proteome analysis and further enzyme-linked immunosorbent assay (ELISA) validation, we observed that calprotectin was independently associated with CV outcome and mortality in 283 patients with CKD or end-stage kidney failure on dialysis. The procalcific role of calprotectin and the therapeutic potential of paquinimod, a specific calprotectin inhibitor, were assessed in primary human VSMCs, mouse aortic rings, and two mouse models of vascular calcification: 5/6 subtotal nephrectomy and in aged apolipoprotein E–deficient ($ApoE^{-/-}$) mice. We further analyzed the link between calprotectin and vascular calcification in an independent cohort of 170 patients with advanced CKD and evaluated in vitro the anticalcifying potential of paquinimod in response to the human uremic milieu.

Table 1. Baseline demographic and biochemical characteristics of the CKD3-4 and the CKD5 Dialysis cohorts. Quantitative variables are presented as medians (IQR). Categorical variables are presented as *n* (%). ARB, angiotensin II receptor blockers; ACEi, angiotensin-converting enzyme inhibitors; BMI, body mass index; Ca × P, calcium phosphate product; eGFR, estimated glomerular filtration rate; PTH, parathyroid hormone.

Parameter	CKD3-4 cohort *n* = 112		CKD5 Dialysis cohort *n* = 171	
Age, year	62	(52–69)	66	(54–75)
Men, *n* (%)	67	(59.8)	96	(56.1)
BMI, kg/m^2	29.5	(26.3–32.8)	25.8	(21.8–30)
CRP, mg/l	3.03	(0.9–6)	4	(1.9–8.6)
eGFR, ml/min per 1.73 m^2	29	(22.2–37.7)	–	
Time on dialysis, year	–		2.7	(1.3–8.8)
Kt/V	–		1.5	(1.4–1.6)
Beta-2-microglobulin, mg/l	–		24.6	(19.7–30.1)
Albumin, g/l	40	(36–43)	37.2	(34.7–39.2)
Hemoglobin, g/dl	12.6	(11.7–14.1)	11.2	(10.2–12)
Calcium (Ca), mM	2.3	(2.2–2.4)	2.2	(2.1–2.3)
Phosphorus (P), mM	1.2	(1.1–1.4)	1.3	(1.1–1.7)
Ca × P, mmol^2/l^2	2.7	(2.4–3.1)	2.9	(2.3–4.1)
PTH, pg/ml	115.5*	(78.2–165.3)	312†	(169–476.5)
Total cholesterol, mM	4.6	(3.9–5.3)	–	
LDL cholesterol, mM	2.7‡	(2–3.1)	2.2†	(1.6–2.6)
HDL cholesterol, mM	1.1‡	(0.9–1.5)	0.9†	(0.7–1.2)
Dyslipidemia, *n* (%)	87	(77.7)	97	(56.7)
Statin, *n* (%)	84	(75)	76	(44.4)
Diabetes, *n* (%)	54	(48.2)	93	(54.4)
Insulin, *n* (%)	38	(33.9)	83	(48.5)
Hypertension, *n* (%)	110	(98.2)	163	(95.3)
ARB/ACEi, *n* (%)	94	(83.9)	73	(42.7)
History of CV events, *n* (%)	0	(0)	70	(40.9)
Smoker, *n* (%)	63	(56.3)	44§	(25.7)

*Data available for 90 of the 112 patients in the CKD3-4 cohort.
†Data available for 92 of the 171 patients in the CKD5 Dialysis cohort.
‡Data available for 102 of the 112 patients in the CKD3-4 cohort.
§Data available for 144 of the 171 patients in the CKD5 Dialysis cohort.

RESULTS

Baseline characteristics of the study population

For this study, we included participants with CKD stage 3 and 4 (CKD3-4) and patients with end-stage kidney failure on dialysis (CKD5 Dialysis). Baseline demographic and clinical characteristics of the patients are summarized in Table 1. The CKD3-4 cohort enrolled 112 patients from the previously described prospective, multicenter cohort study NEFRONA (*13*). The median age was 62 years [interquartile range (IQR), 52 to 69 years]; 67 patients (59.8%) were male, and the median estimated glomerular filtration rate (eGFR) was 29.5 ml/min per 1.73 m^2 (IQR, 22.2 to 37.7 ml/min per 1.73 m^2). At inclusion time, per design of the NEFRONA study, all patients with CKD3-4 were without any history of CV complications. The CKD5 Dialysis cohort included 171 patients with end-stage kidney failure on dialysis from Toulouse and La Reunion (France). The median age was 66 years (IQR, 54 to 75 years); 96

patients (56.1%) were male, and the median time on dialysis was 2.7 years (IQR, 1.3 to 8.8 years).

Serum proteome changes in patients with CKD3-4 with or without CV events

For proteome analysis, we selected a case-control subset of 66 patients from the CKD3-4 cohort. Thirty-two cases who presented a CV event and 34 control patients who did not develop a CV event during follow-up (mean, 3.3 ± 1.2 years) were matched for age, sex, eGFR, diabetes, and cholesterol (Table 2). Controls and cases did not show differences for any other studied baseline characteristic (Table 2). Outcome was a composite end point of fatal (n = 8) and nonfatal (n = 24) CV events.

A total of 443 proteins were identified and quantified in the sera of the patients (table S1). From these, 134 proteins displayed significant (adjusted $P < 0.05$) modified abundance with univariate analysis, 63 with increased and 71 with decreased abundance in patients who developed CV events (Fig. 1A and table S1). Functional enrichment analysis predicted that the 134 deregulated proteins were associated with complement and coagulation systems, negative regulation of endopeptidase activity and proteolysis, and innate immune response (table S2). We also performed a multivariate analysis using random forest (RF) on the 134 deregulated proteins to help identify the most informative proteins. The proteins with the most important fold change (FC ≥ 2 or ≤ 0.5) included epidermal growth factor–containing fibulin-like extracellular matrix protein 2 (*EFEMP2*; FC 13.7), histone H2A type 1-B (*HIST1H2AB*; FC 8.65), calprotectin subunit S100A8 (FC 8.6), and dermcidin (*DCD*; FC 7.63) (Fig. 1B). Calprotectin subunit S100A8 displayed the most significant adjusted P value ($P = 4 \times 10^{-12}$) in univariate analysis and a high RF coefficient in multivariate analysis compared with other protein candidates.

Calprotectin is a 24-kDa heterodimeric DAMP protein formed by S100A8 and S100A9 subunits, two members of the S100 calcium-binding proteins. The abundance of calprotectin subunit S100A9 was also significantly increased ($P = 5 \times 10^{-6}$) in patients who developed CV events compared with patients who did not (Fig. 1B). We observed that both S100A8 and S100A9 subunits displayed similar correlation patterns with the other most strongly deregulated proteins (Fig. 1C). The abundance of S100A8 was strongly correlated with the abundance of S100A9 in the serum proteome of patients with CKD (Spearman $r = 0.62$, $P < 0.0001$ and $r = 0.58$, $P = 0.0005$ in patients without and with CV event, respectively; Fig. 1, D and E), suggesting heterodimer association of the two subunits as calprotectin.

Table 2. Baseline demographic and biochemical parameters of the CKD3-4 subcohort used for proteome analysis. Quantitative variables are presented as medians (IQR). Categorical variables are presented as n (%).

Parameter	Subcohort n = 66		Controls n = 34		Cases n = 32		P
Age, year	**66**	**(59–70)**	**66**	**(61–71)**	**64**	**(54–70)**	**0.18**
Men, n (%)	47	(71.2)	25	(73.5)	22	(68.7)	0.67
BMI, kg/m^2	30.11	(27.3–32.8)	29.2	(27.3–32.1)	30.9	(25.9–34.3)	0.57
CRP, mg/l	2.87	(0.9–6.5)	3.04	(0.9–6.0)	2.83	(1.4–7.0)	0.36
eGFR, ml/min per 1.73 m^2	29	(22.2–37.6)	29	(22.3–37.8)	28	(21.1–37.6)	0.72
Albumin, g/l	40	(36–43)	39.5	(36–43)	40	(36–43)	0.79
Hemoglobin, g/dl	12.6	(11.9–14.6)	12.7	(11.9–14.6)	12.4	(11.6–15)	0.88
Calcium (Ca), mM	2.3	(2.2–2.4)	2.3	(2.2–2.4)	2.3	(2.2–2.4)	0.44
Phosphorus (P), mM	1.2	(1.1–1.4)	1.2	(1.0–1.4)	1.2	(1.1–1.4)	0.20
Ca × P, mmol^2/l^2	2.7	(2.4–3.2)	2.7	(2.4–3.1)	2.9	(2.6–3.3)	0.15
PTH, pg/ml	119*	(70.5–173)	107.5	(68.5–157.5)	121	(76–200.8)	0.33
Total cholesterol, mM	4.5	(3.8–5.3)	4.4	(3.8–5.5)	4.6	(4.0–5.4)	0.87
LDL cholesterol, mM	2.7†	(2–3.1)	2.6	(2–3.3)	2.8	(1.9–3.2)	0.81
HDL cholesterol, mM	1.1†	(0.9–1.4)	1.1	(0.9–1.3)	1.1	(0.9–1.5)	0.52
Dyslipidemia, n (%)	53	(80.3)	27	(79.4)	26	(81.2)	0.85
Statin, n (%)	46	(69.7)	24	(70.6)	22	(68.7)	0.87
Diabetes, n (%)	41	(62.1)	22	(64.7)	19	(59.4)	0.66
Insulin, n (%)	30	(45.5)	16	(47.1)	14	(43.7)	0.79
Hypertension, n (%)	66	100	34	(100)	32	(100)	–
ARB/ACEi, n (%)	59	(89.4)	29	(85.3)	30	(93.7)	0.26
Smoker, n (%)	41	(62.1)	22	(64.7)	19	(59.4)	0.66

*Data available for 55 of the 66 patients in the CKD3-4 subcohort. †Data available for 59 of the 66 patients in the CKD3-4 subcohort.

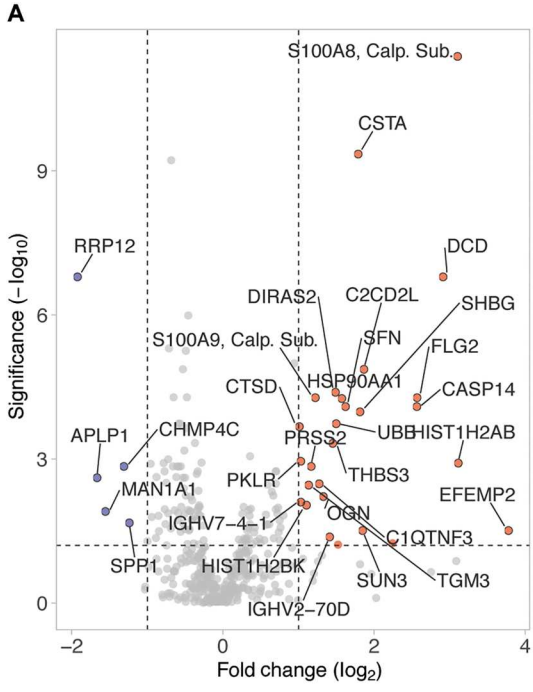

B

Gene name	Description	Fold change	Adjusted *P*	RF coeff.
S100A8	**Protein S100-A8, Calp. Sub.**	8.6	4.10^{-12}	13.3
CSTA	Cystatin-A	3.45	4.10^{-10}	15.3
DCD	Dermcidin	7.52	2.10^{-7}	11.6
C2CD2L	Phospholipid transfer protein C2CD2L	3.64	1.10^{-5}	11.6
DIRAS2	GTP-binding protein Di-Ras2	2.81	4.10^{-5}	7.5
FLG2	Filaggrin-2	5.93	5.10^{-5}	6.5
S100A9	**Protein S100-A9, Calp. Sub.**	2.33	5.10^{-5}	6.1
HSP90AA1	Heat shock protein HSP 90-alpha	2.97	5.10^{-5}	7.5
CASP14	Caspase-14	5.92	8.10^{-5}	8.0
SFN	14-3-3 protein sigma	3.08	8.10^{-5}	10.7
SHBG	Sex hormone-binding globulin	3.51	1.10^{-4}	4.7
UBB	Polyubiquitin-B	2.82	2.10^{-4}	13.5
CTSD	Cathepsin D	2.01	2.10^{-4}	3.8
THBS3	Thrombospondin-3	2.74	5.10^{-4}	10.0
PKLR	Pyruvate kinase PKLR	2.04	1.10^{-3}	6.4
HIST1H2AB	Histone H2A type 1-B/E	8.65	1.10^{-3}	4.1
PRSS2	Trypsin-2	2.24	1.10^{-3}	8.4
C1QTNF3	Complement C1q tumor necrosis factor-related protein 3	2.42	3.10^{-3}	5.2
TGM3	Protein-glutamine gamma-glutamyltransferase E	2.19	3.10^{-3}	2.3
OGN	Mimecan	2.51	6.10^{-3}	3.4
HIST1H2BK	Histone H2B type 1-K	2.15	9.10^{-3}	0.4
EFEMP2	EGF-containing fibulin-like extracellular matrix protein 2	13.71	3.10^{-2}	4.4
SUN3	SUN domain-containing protein 3	3.6	3.10^{-2}	6.5
RRP12	RRP12-like protein	0.26	1.10^{-7}	10.1
CHMP4C	Charged multivesicular body protein 4c	0.40	1.10^{-3}	3.3
APLP1	Amyloid-like protein 1	0.32	2.10^{-3}	3.1
MAN1A1	Mannosyl-oligosaccharide 1,2-alpha-mannosidase IA	0.34	1.10^{-2}	2.3
SPP1	Osteopontin	0.42	2.10^{-2}	4.5

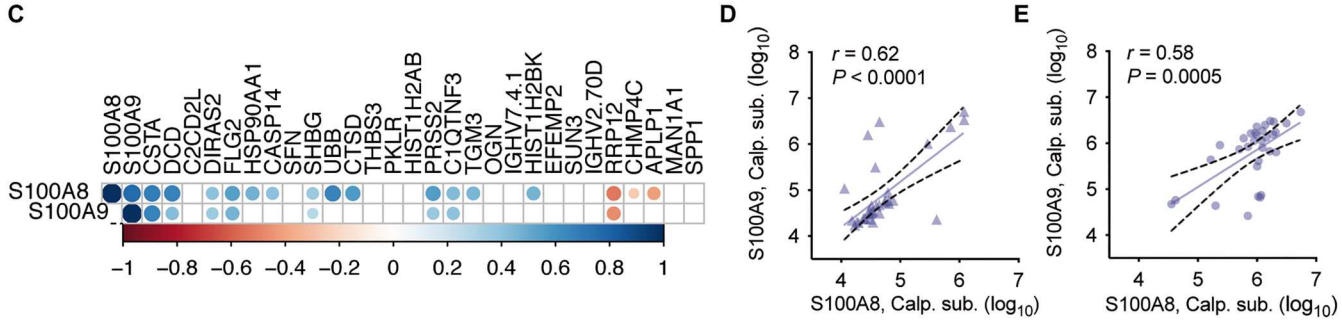

Fig. 1. Serum proteome analysis of patients with CKD3-4. (**A**) Volcano plot of differences in abundance in the serum proteome between patients who presented a major CV event (n = 32) compared with those who did not present with a CV complication (n = 34). Colored dots represent proteins with increased (red) or decreased (blue) abundance with adjusted $P < 0.05$ (Student's t test adjusted using Benjamini-Hochberg). Labeled dots represent proteins with fold change ≥2 or ≤0.5 [$-2 \geq \log_2$(fold change) ≥ 2] and adjusted $P < 0.05$ with Student's t test adjusted using Benjamini-Hochberg. (**B**) Univariate and multivariate feature ranking using RF analysis of the deregulated serum proteins associated with severe outcome [$-2 \geq \log_2$(fold change) ≥ 2 and adjusted $P < 0.05$]. (**C**) Pearson correlation plot of S100A8 and S100A9 calprotectin subunits with the other deregulated serum proteins associated with severe outcomes [$-2 \geq \log_2$(fold change) ≥ 2 and adjusted $P < 0.05$]. (**D**) Pearson correlation of the $\log_{10}$ serum proteomic abundance of S100A8 and S100A9 calprotectin subunits in patients without a major CV event. (**E**) Pearson correlation of the $\log_{10}$ serum proteomic abundance of S100A8 and S100A9 calprotectin subunits in patients with a major CV event. Calp. sub., calprotectin subunit; RF, random forest.

Association of circulating calprotectin with CV outcome in patients with CKD and on dialysis

To validate these findings, we next measured circulating calprotectin using ELISA in the full CKD3-4 cohort (n = 112) and CKD5 Dialysis cohort (n = 171). In both cohorts, circulating calprotectin concentration was positively associated with C-reactive protein (CRP) using univariate and multivariate linear regression (tables S3 and S4). In the CKD5 Dialysis cohort, calprotectin also showed a significant inverse correlation with serum albumin (P = 0.003) using univariate analysis, but the association was lost in multivariate analysis because of the colinearity of serum albumin with CRP. Calprotectin also showed a weak but significant association with calcium phosphate product (Ca × P; P = 0.03; table S4).

The CKD3-4 cohort registered 39 CV events during follow-up (mean, 3.5 ± 1.1 years): 9 were fatal, and 30 were nonfatal CV events. The CKD5 Dialysis cohort registered 42 fatal or nonfatal CV events during follow-up (mean, 1.6 ± 0.6 years). In both cohorts, mortality and CV events were associated with higher baseline circulating calprotectin (Fig. 2, A and B). These differences remained significant after adjusting for CRP (P = 0.001) or age, male sex, and diabetes ($P < 0.001$). The relationship between circulating calprotectin and future occurrence of fatal or nonfatal events was estimated by time-to-event analysis. Patients in the CKD3-4 and CKD5 Dialysis cohorts were stratified according to baseline serum and plasma calprotectin tertiles, respectively. Higher calprotectin tertiles were associated with higher CRP concentrations in both cohorts (P = 0.05 in CKD3-4 and P = 0.04 in CKD5 Dialysis) but

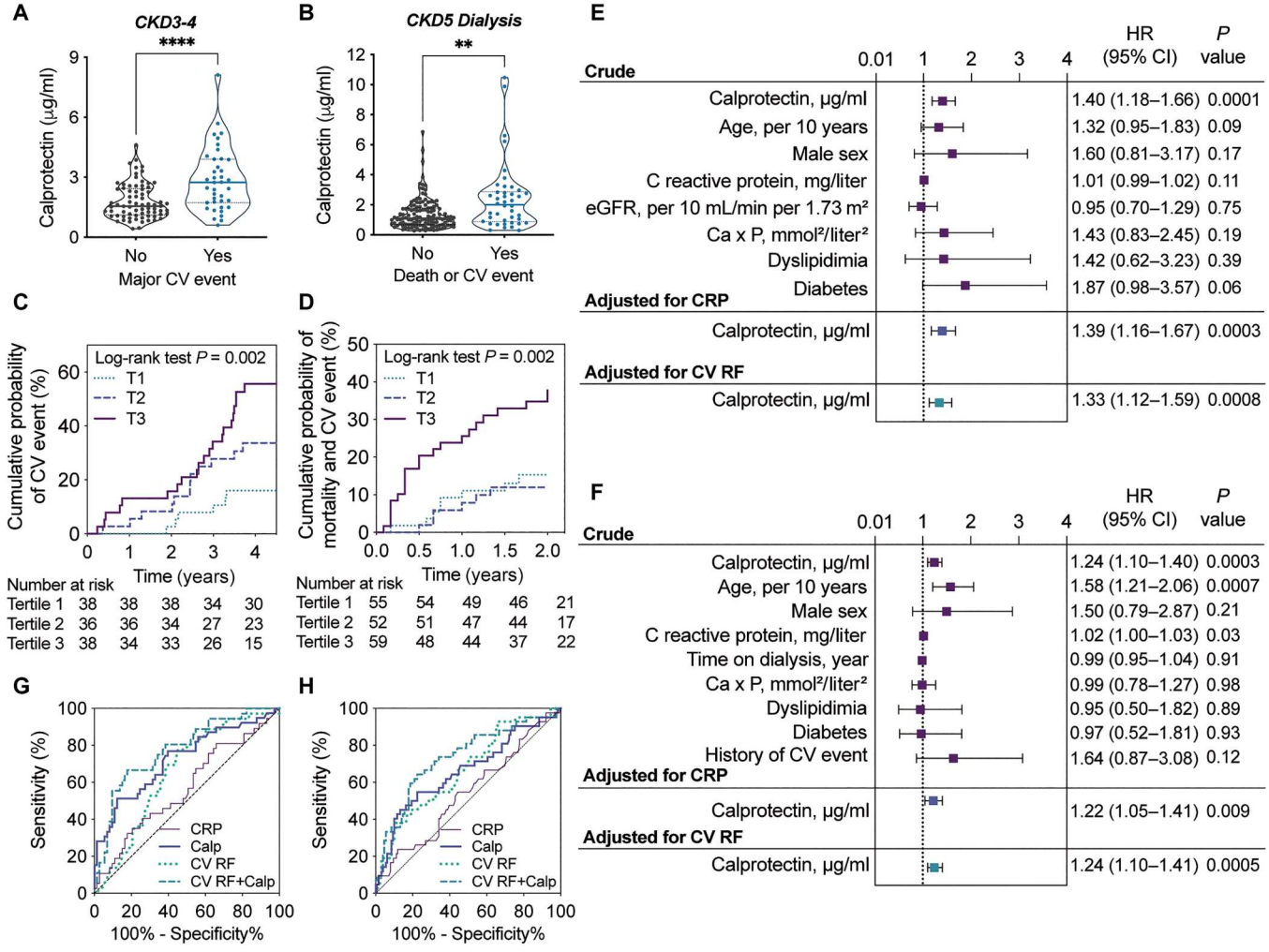

Fig. 2. Circulating calprotectin associates with outcome in patients with CKD3-4 and in patients with CKD5 on dialysis. (**A** and **B**) Circulating calprotectin concentrations measured by ELISA in the sera of patients with CKD3-4 who presented with a major CV event (n = 39) compared with those who did not develop any CV complications (n = 73) (A) and in the plasma of patients with CKD5 on dialysis with (n = 42) or without (n = 129) mortality or CV event (B). $^{**}P < 0.01$ and $^{****}P < 0.0001$ by unpaired Mann-Whitney U test. (**C** and **D**) Kaplan-Meier estimate of probability of a first major CV event in patients with CKD3-4 (C) and of mortality risk or CV event in patients with CKD5 on dialysis (D) according to circulating calprotectin concentration at the time of inclusion when patients were grouped on the basis of calprotectin tertiles. Tertile cutoff for CKD3-4: tertile 1, <1.43 µg/ml; tertile 2, 1.43 to 2.46 µg/ml; tertile 3, >2.46 µg/ml. Tertile cutoff for CKD5 Dialysis: tertile 1, <0.90 µg/ml; tertile 2, 0.90 to 1.74 µg/ml; tertile 3, >1.74 µg/ml. Number at risk: number of patients still followed at the indicated time. (**E** and **F**) Association of calprotectin with CV outcome in patients with CKD3-4 (E) and with mortality and CV event in patients with CKD5 on dialysis (F) using univariate and multivariate Cox regression analyses. Multivariate analyses were adjusted for C-reactive protein (CRP) or cardiovascular risk factors (CV RF), including age, sex, and diabetes. (**G** and **H**) Receiver operating characteristics curves for prediction of CV outcome in patients with CKD3-4 (G) and of mortality and CV event in patients with CKD5 on dialysis (H) for calprotectin concentration (Calp), CRP, and for multivariable regression models including CV RFs (age, male sex, and diabetes) without (CV RF) or with calprotectin (CV RF + Calp). HR, hazard ratio; CI, confidence interval.

did not show any association with other baseline parameters such as age, sex, or serum phosphate (tables S5 and S6). The cumulative probability of mortality and CV event was significantly higher in the third tertile of calprotectin concentration group in both cohorts (6 events in tertile 1, 12 in tertile 2, and 21 in tertile 3, log-rank, P = 0.002 for CKD3-4 and 11 events in tertile 1, 7 in tertile 2, and 22 in tertile 3, log-rank, P = 0.002 for CKD5 Dialysis; Fig. 2, C and D).

Univariate and multivariate Cox proportional hazard analyses were performed to study the effect of calprotectin concentration, used as a continuous variable, with or without traditional confounding factors, on the probability of developing a major event. In univariate Cox analysis, calprotectin was associated with a higher risk of mortality and CV event in patients in the CKD3-4 (Fig. 2E) and CKD5 Dialysis (Fig. 2F) cohorts. Other baseline parameters associated with severe outcome were age, CRP, and diabetes (Fig. 2, E and F). The association of calprotectin with outcome was still observed after adjustment for CRP or conventional CV risk factors (CV RFs), including age, sex, and diabetes (Fig. 2, E and F).

Last, we assessed the performance of calprotectin, CRP, and CV RFs such as age, male sex, and diabetes as predictors of outcome in patients with CKD. In both cohorts, calprotectin showed prognostic

Table 3. Baseline demographic and biochemical characteristics in the full CKD5 cohort or in patients grouped according to serum calprotectin concentration. Calprotectin concentration cutoff: <1.43 μg/ml, 1.43 to 2.46 μg/ml, and >2.46 μg/ml, based on CKD3-4 tertile thresholds. Quantitative variables are presented as medians (IQR). Categorical variables are presented as *n* (%).

			Serum calprotectin						
Parameter	**CKD5 cohort *n* = 191**		**<1.43 μg/ml *n* = 47**		**1.43–2.46 μg/ml *n* = 70**		**>2.46 μg/ml *n* = 74**		***P***
Age, year	47	(32–55)	48	(34–55)	44	(30–57)	46	(36–55)	0.97
Men, *n* (%)	119	(70%)	33	(70%)	50	(71%)	57	(77%)	0.64
BMI, kg/m^2	24.2	(22.5–26.5)	24	(23–26)	24	(22–27)	24	(22–28)	0.71
CRP, mg/l	0.9	(0.3–2.2)	0.8	(0.4–1.6)	0.7	(0.3–1.6)	1	(0.3–3.1)	0.59
Albumin, g/l	35	(32–37)	35	(33–37)	35	(32–37)	34	(32–38)	0.69
Hemoglobin, g/dl	11.5	(10.8–12.5)	11.6	(10.9–12.1)	11.7	(10.5–12.7)	11.3	(10.5–12.1)	0.36
Calcium (Ca), mM	2.3	(2.1–2.4)	2.3	(2.2–2.4)	2.3	(2.2–2.4)	2.3	(2.1–2.4)	0.22
Phosphorus (P), mM	1.7	(1.4–2)	1.6	(1.3–1.8)	1.7	(1.3–2.1)	1.6	(1.4–2.0)	0.27
Ca × P, mmol^2/l^2	3.8	(3.1–4.5)	3.6	(3.1–4.1)	4.0	(3.1–4.6)	3.5	(3.0–4.4)	0.29
PTH, pg/ml	25	(16–40)	25	(20.4–37)	27	(17–47)	21.5	(12–37.7)	0.18
Total cholesterol, mM	4.4	(3.7–5.2)	4.4	(3.6–4.9)	4.6	(3.7–5.6)	4.2	(3.5–5)	0.08
HDL cholesterol, mM	1.3	(1–1.6)	1.3	(1–1.6)	1.3	(1.1–1.6)	1.2	(1–1.6)	0.47
Diabetes, *n* (%)	13*	(9.8%)	5	(13%)	3	(6%)	5	(11%)	0.54
Vascular calcification, *n* (%)	143	(75%)	29	(61%)	51	(73%)	63	(85%)	0.01

*Data available for 133 patients.

value with an area under the receiver operating characteristic curve (AUC) of 0.72 and 95% confidence interval (CI) of 0.62 to 0.83 in the CKD3-4 cohort ($P < 0.0001$; Fig. 2G) and an AUC of 0.66 and 95% CI of 0.56 to 0.76 in the CKD5 Dialysis cohort ($P = 0.002$; Fig. 2H). CRP concentrations did not show any discriminatory ability (CKD3-4: AUC, 0.57 and $P = 0.24$; CKD5 Dialysis: AUC, 0.54 and $P = 0.43$; Fig. 2, G and H). Using multivariate logistic regression, we developed additional models including CV RF alone or in combination with calprotectin (CV RF + Calp). In the CKD3-4 cohort, CV RF predicted an outcome with an AUC of 0.65 ($P = 0.008$), and adding calprotectin to CV RF substantially improved the accuracy of CV event prediction (AUC, 0.77 and $P < 0.0001$; $P < 0.05$ compared with CV RF alone; Fig. 2G). Similar results were obtained in the CKD5 Dialysis cohort with an AUC of 0.67 for CV RF alone ($P = 0.001$) and an AUC of 0.73 ($P < 0.0001$) for CV RF with calprotectin ($P < 0.05$ compared with CV RF alone; Fig. 2H).

Association of circulating calprotectin with vascular calcification in patients with CKD

To obtain further clinical evidence of the association between circulating calprotectin and medial vascular calcification in CKD, we measured calprotectin concentrations in the sera of 191 patients with CKD5 undergoing living-donor kidney transplantation. Vascular calcification was assessed through Von Kossa staining in epigastric artery sections collected during renal transplantation surgery. Baseline demographic and clinical characteristics of the patients (before transplantation), as well as biochemical parameters, are summarized in Table 3. In univariate and multivariate analysis, circulating calprotectin showed no association with any clinical and biochemical parameters at baseline (table S7). Baseline serum calprotectin concentration was measured using ELISA. Patients were then grouped according to the tertile concentration thresholds determined in the CKD3-4 cohort. Higher concentrations of serum calprotectin were associated with a significant increase in vascular calcification ($P = 0.01$) in these patients (Table 3).

Effect of calprotectin on vascular calcification in vitro

To study the role of calprotectin in vascular calcification, we investigated whether calprotectin could promote calcification in primary human aortic smooth muscle cells (hASMCs) and in mouse aortic rings. Treatment with phosphate (Pi)–containing calcification medium induced calcium deposition in hASMCs (Fig. 3A) and in mouse aortic rings (Fig. 3B). This effect was enhanced after additional treatment with recombinant calprotectin (10 μg/ml; Fig. 3, A and B). Calprotectin did not induce calcium deposition in hASMCs and in mouse aortic rings cultivated in control medium in the absence of Pi (fig. S1). To elucidate the underlying mechanisms of calprotectin-induced calcification, we investigated the implication of the two known receptors of calprotectin, Toll-like receptor 4 (TLR4) and the receptor for advanced glycation end products (RAGE). In hASMCs, blocking of TLR4 and RAGE receptors using the TLR4 inhibitor TAK-242 (3 μM; Fig. 3C) or anti-RAGE blocking antibody (10 μg/ml; Fig. 3D) abrogated calcium deposition induced by calprotectin compared with vehicle or isotype control immunoglobulin, respectively. Treatment of hASMCs with TAK-242 or anti-RAGE blocking antibody did not modify calcium deposition induced by calcification medium (Pi) in the absence of calprotectin (Fig. 3, C and D).

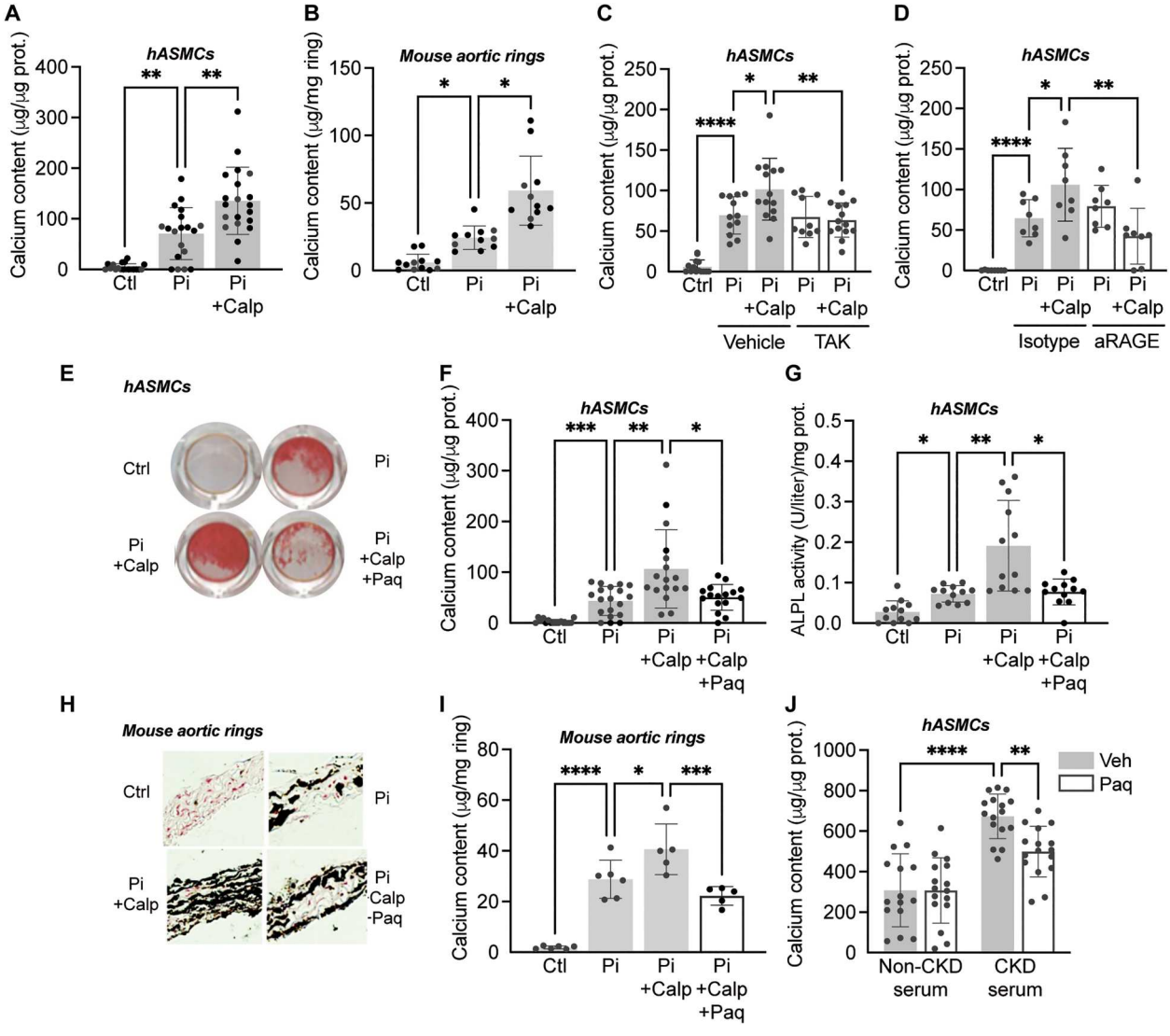

Fig. 3. Effect of calprotectin and paquinimod on vascular calcification in hASMCs and mouse aortic rings. (**A** and **B**) Calcium content in primary hASMCs (n = 19 or 20 per group) (A) and mouse aortic rings (n = 11 or 12 per group) (B) cultivated in control (Ctrl) or calcification medium (Pi) and treated or not with calprotectin (10 µg/ml; Calp). (**C** and **D**) Calcium content in hASMCs cultivated in control (Ctrl) or calcification medium (Pi) and treated or not with calprotectin (10 µg/ml; Calp) and 3 µM TAK-242 (TAK) or vehicle (n = 10 to 14 per group) (C) or anti-RAGE blocking antibody (10 µg/ml; aRAGE) or isotype control immunoglobulin (n = 8 per group) (D). (**E** to **G**) Alizarin red staining (E), calcium content (n = 16 to 19 per group) (F), and ALPL activity (n = 12 per group) (G) in hASMCs and cultivated in control (Ctrl) or calcification medium (Pi) and treated or not with calprotectin (10 µg/ml; Calp) and paquinimod (10 µg/ml; Paq). (**H** and **I**) Von Kossa staining (H) and calcium content (n = 5 or 6 per group) (I) in mouse aortic rings cultivated in control (Ctrl) or calcification medium (Pi) and treated or not with calprotectin (10 µg/ml; Calp) and paquinimod (10 µg/ml; Paq). (**J**) Calcium content in hASMCs treated with normal serum collected from individuals without CKD or uremic serum collected from patients with CKD5 and with additional treatment with vehicle or paquinimod (10 µg/ml; n = 15 or 16 per group). *P < 0.05, **P < 0.01, ***P < 0.001, and ****P < 0.0001 by Kruskal-Wallis test with Dunn's multiple comparisons for (A to G), one-way ANOVA test with Šidák's multiple comparisons for (I), or two-way ANOVA test with Tukey's multiple comparisons for (J). Error bars represent SDs of the mean.

Effect of calprotectin blockade with paquinimod on vascular calcification in vitro

We next evaluated the potential of calprotectin as a possible therapeutic target in vascular calcification in vitro. To this end, hASMCs and mouse aortic rings were treated with phosphate and calprotectin without or with additional treatment with the calprotectin inhibitor paquinimod (10 µg/ml). In hASMCs, paquinimod alleviated increased calprotectin-induced calcification assessed by alizarin red staining (Fig. 3E), calcium content (Fig. 3F), and ALPL activity (Fig. 3G). Similar results were observed in mouse aortic rings using Von Kossa staining and calcium content measurement (Fig. 3, H and I). Treatment of hASMCs with paquinimod did not modify calcium deposition induced by calcification medium (Pi) alone in the absence of calprotectin (fig. S2).

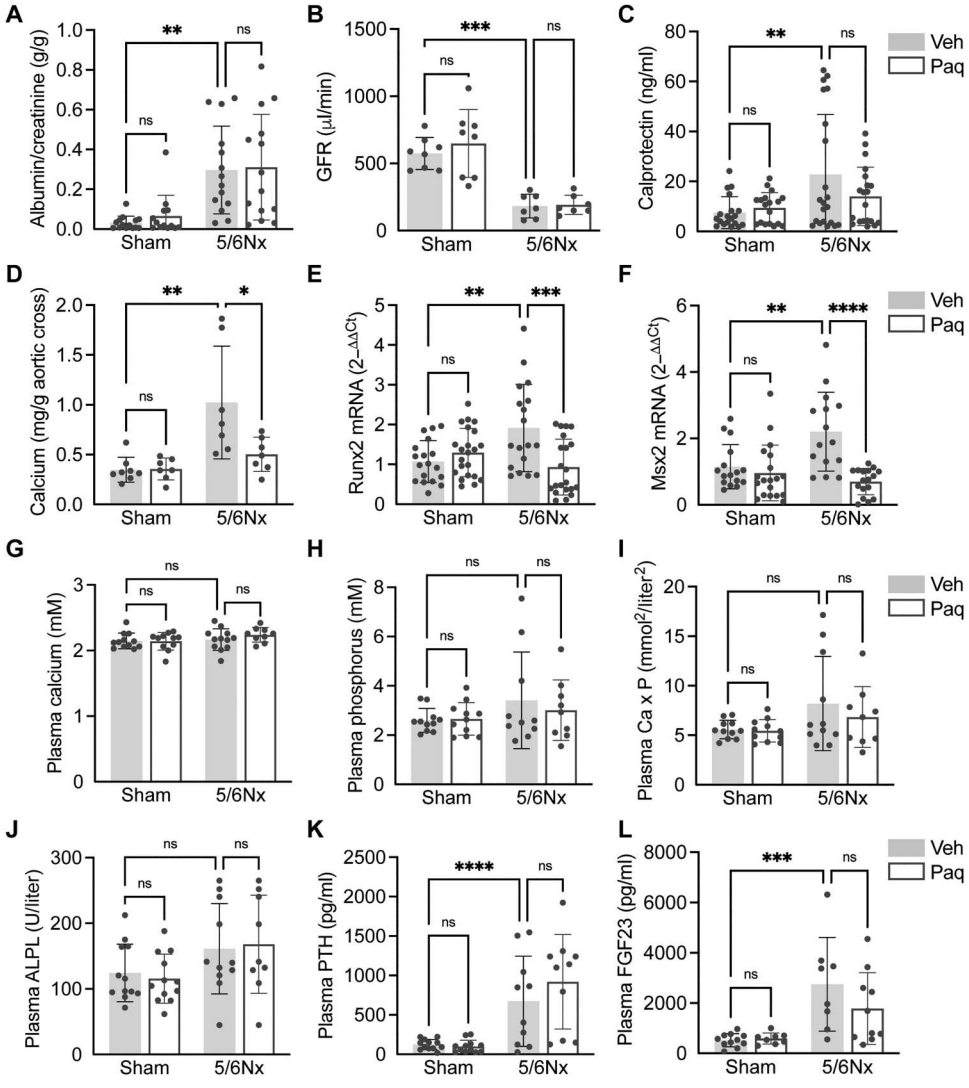

Fig. 4. Paquinimod treatment reduces vascular calcification in 5/6 Nx mice. (**A**) Urinary albumin/creatinine ratio ($n = 14$ per group), (**B**) GFR ($n = 7$ or 8 per group), (**C**) plasma calprotectin concentration ($n = 18$ to 21 per group), (**D**) calcium content in the aortic cross ($n = 7$ or 8 per group) of sham, and 5/6 Nx mice treated with vehicle or paquinimod. (**E**) *Runx2* and (**F**) *Msx2* mRNA expression ($n = 15$ to 22 per group) in the thoracic aortas of sham and 5/6 Nx mice treated with vehicle or paquinimod. (**G**) Plasma calcium (Ca), (**H**) plasma phosphorus (P), (**I**) plasma Ca × P, (**J**) plasma ALPL activity, (**K**) plasma PTH, and (**L**) plasma FGF23 concentrations ($n = 8$ to 12 per group) of sham and 5/6 Nx mice treated with vehicle or paquinimod. *$P < 0.05$, **$P < 0.01$, ***$P < 0.001$, and ****$P < 0.0001$ by two-way ANOVA test with Tukey's multiple comparisons for (A to K). Error bars represent SDs of the mean. ns, not significant.

Effect of paquinimod on vascular calcification induced by human uremic serum in vitro

To increase the translational value of our observations, we explored the therapeutic potential of paquinimod in the complex uremic milieu. hASMCs exposed to uremic serum from patients with CKD5 or to serum collected from individuals without CKD were treated or not with paquinimod. The calcium content was increased in hASMCs exposed to uremic serum compared with serum from non-CKD controls, and this effect was reduced after treatment with paquinimod (Fig. 3J).

Effect of paquinimod on vascular calcification in a subtotal nephrectomy mice model

The anticalcifying effect of paquinimod was further evaluated in phosphate-fed DBA (dilute, brown, non-agouti) mice subjected to subtotal nephrectomy (5/6 Nx), a clinically relevant model of vascular calcification associated with CKD. Subtotal nephrectomy increased albuminuria (Fig. 4A) and decreased measured GFR (Fig. 4B), confirming kidney disease in the 5/6 Nx mice compared with the sham control mice. In addition, plasma calprotectin concentrations were increased in 5/6 Nx mice treated with vehicle compared with the sham control mice (Fig. 4C). Increased plasma calprotectin concentrations were correlated to GFR decline and increased monocyte count (fig. S2). In addition, in 5/6 Nx mice, phosphate-rich diet increased plasma calprotectin concentrations compared with

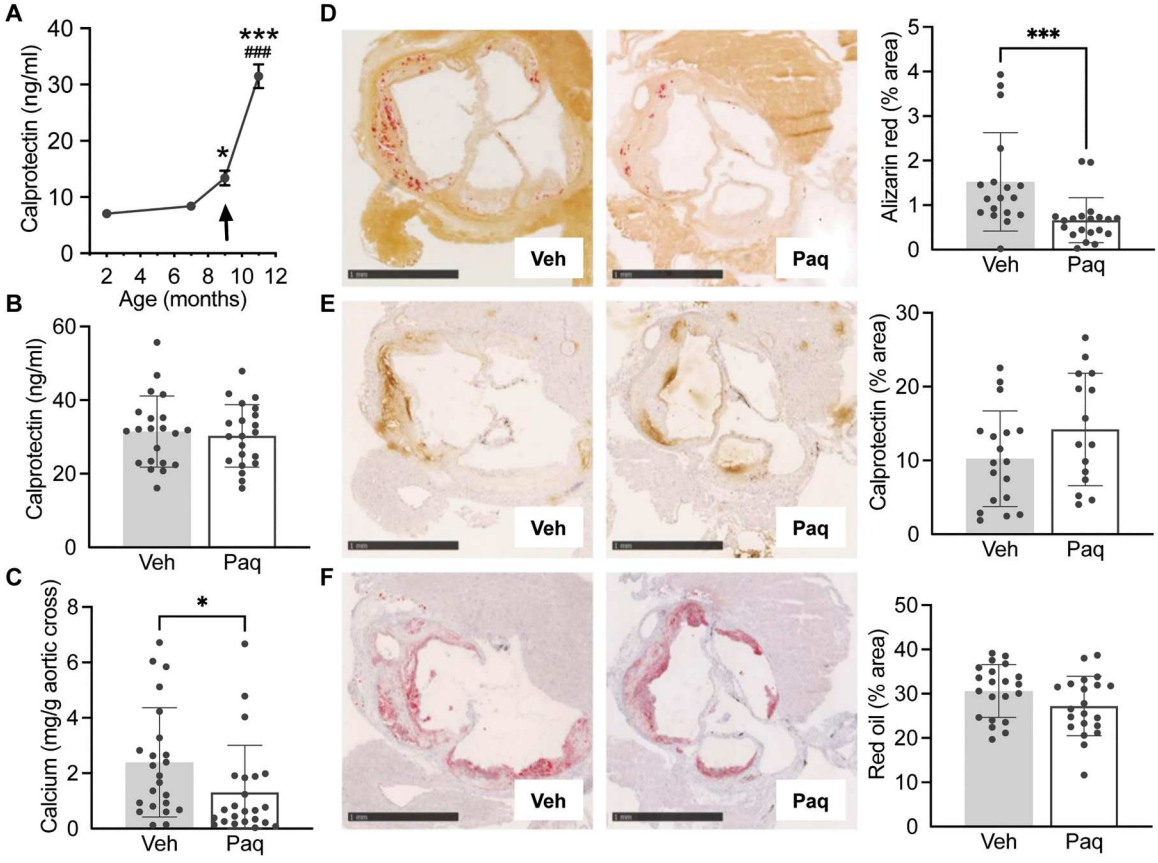

Fig. 5. Paquinimod treatment reduces vascular calcification in old ApoE$^{-/-}$ mice. (**A**) Plasma calprotectin concentrations measured in ApoE$^{-/-}$ mice fed with a normal diet for 9 months before switching to high-phosphate diet (arrow). *P < 0.05 and ***P < 0.001 compared with 2 months old; ###P < 0.001 compared with 9 months old by Kruskal-Wallis test with Dunn's multiple comparisons. (**B**) Plasma calprotectin concentrations (n = 21 per group), (**C**) calcium content in the aortic cross (n = 23 per group). (**D** to **F**) Representative images and quantification (n = 18 to 21 per group) of (D) alizarin red (calcium deposition), (E) calprotectin, and (F) red oil staining (lipid accumulation) on the aortic sinus in 11-month-old ApoE$^{-/-}$ mice treated with vehicle (Veh) or paquinimod (Paq) for 8 weeks. Scale bars, 1 mm. **P < 0.01 and ***P < 0.001 by unpaired Mann-Whitney U test for (B to F). Error bars represent SDs of the mean.

normal diet without modifying GFR or modifying monocyte count (fig. S3). Mice with subtotal nephrectomy on a phosphate-rich diet also showed increased calcification of the aortic arch (Fig. 4D) and aortic mRNA expression of osteogenic markers *Runx2* and *Msx2* (Fig. 4, E and F). Treatment with paquinimod for 8 weeks prevented the development of vascular calcification (Fig. 4, D to F) without modifying renal function (Fig. 4, A and B) or plasma calprotectin concentration (Fig. 4C). To assess the impact of 5/6 Nx and paquinimod on bone mineral metabolism, we measured plasma concentrations of calcium (Ca), phosphorus (P), ALPL, intact parathyroid hormone (PTH), and fibroblast growth factor 23 (FGF23; C-terminal fragment; Fig. 4, G to L). Both PTH and FGF23 were increased in the plasma of 5/6 Nx mice treated with the vehicle compared with sham, but paquinimod did not affect any of these markers (Fig. 4, K and L).

Effect of paquinimod on vascular calcification in old ApoE$^{-/-}$ mice

We next evaluated the potential protective effect of paquinimod in a different complex pathological context associated with vascular calcification combining atherosclerosis and aging. In ApoE$^{-/-}$ mice, aging was associated with increased plasma calprotectin (Fig. 5A). To further potentiate the development of calcification, 9-month-old ApoE$^{-/-}$ mice were fed a phosphate-rich diet, substantially increasing plasma calprotectin (Fig. 5A), and treated or not with paquinimod for 8 weeks. Treatment with paquinimod did not modify plasma calprotectin concentrations (Fig. 5B) but did reduce calcium content of the aortic cross (Fig. 5C) compared with vehicle. Eleven-month-old ApoE$^{-/-}$ mice treated with vehicle displayed atherosclerotic plaques complicated by intimal microcalcifications as shown by alizarin red staining of the aortic sinus (Fig. 5D). These lesions were associated with intraplaque calprotectin staining (Fig. 5E). Treatment with paquinimod reduced plaque calcification (Fig. 5D) without modifying plaque calprotectin staining (Fig. 5E) or the size of the plaque (Fig. 5F) compared to vehicle.

DISCUSSION

CV disease is the main cause of death in patients with CKD worldwide, and vascular calcification is a strong predictor for mortality in these patients. In this study, we identified calprotectin as associated with CV outcome and mortality in patients with CKD and as a potential therapeutic target to prevent vascular calcification.

Calprotectin is a marker of disease activity in many autoimmune and inflammatory diseases, including rheumatoid arthritis, inflammatory bowel disease, systemic lupus erythematous, or, more recently, COVID-19 (*14*–*16*). Some reports have shown that circulating calprotectin was increased in dialysis patients compared with healthy individuals (*17*, *18*) and that serum calprotectin was associated with overall mortality in hemodialysis patients with elevated serum phosphorus or patients on peritoneal dialysis (*19*, *20*). In addition, increased circulating calprotectin has been associated with a higher incidence of CV events in patients without CKD, including coronary events, peripheral arterial disease, and acute ischemic stroke (*21*–*24*). However, few reports have suggested that calprotectin may have a direct effect on the CV system in vivo.

Primarily expressed and secreted by myeloid-derived cells such as neutrophils and monocytes, calprotectin may be released into the extracellular space by other cells upon activation, injury, or death (*14*, *15*). In the extracellular environment, calprotectin becomes a proinflammatory mediator, serving as a DAMP or a so-called alarmin. Calprotectin stimulates oxidative stress, production of inflammatory cytokines, and apoptosis upon interaction with TLR4 and RAGE (*14*, *15*), which have both already been described to play a role in vascular calcification (*25*, *26*). The S100A9-RAGE axis has also been shown to promote the release of macrophage-mediated mineralizing extracellular vesicles under hyperglycemic conditions (*27*). Nevertheless, knowledge of calprotectin signaling in VSMCs is limited. Here, we showed that calprotectin promotes calcification of VSMCs through TLR4 and RAGE. We showed that the activity of ALPL, a key end-effector induced by procalcific pathways, was increased by calprotectin, demonstrating the effect of calprotectin on osteogenic processes at the functional level. Further studies are needed to better understand the molecular and cellular mechanisms associated with calprotectin's procalcifying effects on VSMCs, including senescence, apoptosis, release of calcifying microvesicles, and inflammatory cytokine production.

Given the close link between calprotectin and inflammation, it might be assumed that calprotectin accumulation may reflect or mediate the inflammatory state that characterizes CKD and might therefore explain the relationship between increased circulating calprotectin and vascular calcification and CV mortality in patients with CKD. Chronic inflammation and the acute phase inflammatory response, characterized by higher CRP and interleukin-6 and lower albumin, are predictors of early mortality in patients with end-stage kidney failure and dialysis (*28*). In our study, calprotectin was correlated with CRP in CKD stages 3 and 4 and in dialysis patients but not in the selected group of patients with CKD5 undergoing living-donor transplantation. In addition, calprotectin was more strongly and independently associated with CV outcome and mortality than CRP. Our results, in accordance with previous reports (*17*, *19*, *20*, *24*), suggest that the regulation of calprotectin and CRP respond to different mechanisms and that calprotectin may be a more sensitive marker of the chronic inflammatory state than CRP. In our 5/6 Nx mouse model, increased plasma calprotectin was strongly correlated to renal function decline and monocyte count. The phosphate-rich diet also increased plasma calprotectin, independently of an effect on renal function or inflammatory cells. Therefore, it could be hypothesized that in the context of chronic systemic inflammation associated with renal failure and phosphate dysregulation, higher circulating calprotectin results from decreased renal elimination and increased production by inflammatory cells, although additional stress factors could also have a direct effect on other cell types to release calprotectin as an alarmin. Future studies are needed to identify the cellular source of calprotectin during calcification conditions, including inflammatory cells, VSMCs, and endothelial cells.

Clinical management of vascular calcification in patients with CKD currently relies on the prevention of mineral metabolism disorders, but this does not result in a major change to the rate of progression (*7*, *11*). Experimental therapies, such as bisphosphonates, thiosulfates, or lowering pH, were successful in animal models, but their efficacy in humans is still debated or remains to be proven (*7*, *11*). Paquinimod (ABR 215757) is an orally administered drug belonging to the class of quinoline-3-carboxamides, a class of small compounds with immunomodulatory properties (*29*). Paquinimod has been granted the status of an orphan drug by the Food and Drug Administration and has been demonstrated safe in phase 1 and 2 clinical trials in the treatment of lupus and systemic sclerosis, as well as in several animal models of atherosclerosis, myocardial infarction, autoimmune encephalomyelitis, and skin fibrosis. Although its mode of action remains incompletely understood, it has been shown that paquinimod competes for the same binding region in calprotectin as TLR4 and RAGE, without binding directly to the receptors and without directly regulating calprotectin expression (*29*). This is supported by our models, where paquinimod reduced vascular calcification without modifying calprotectin abundance in the plasma of 5/6 Nx and $ApoE^{-/-}$ mice or in the atherosclerotic plaque of $ApoE^{-/-}$ mice. Although our results suggest that paquinimod did not aggravate bone mineral disorder associated with renal failure in the 5/6 Nx mouse model, additional studies are warranted to explore in more detail the potential side effects of paquinimod that may directly affect the bone formation and its mineral density.

In addition to calprotectin, our proteomics analysis identified more than 100 proteins associated with CV outcome in patients with CKD. Among those, plasminogen activator inhibitor 1, mimecan, and cathepsin D have already been shown to be associated with CKD-associated CVD (*30*–*32*). Fetuin A (alpha-2-HS glycoprotein), a circulating glycoprotein derived from the liver, is a well-known and potent inhibitor of calcification, and decreased fetuin A concentrations have been associated with an increased risk of mortality in patients on dialysis (*33*). However, in our study, although detected in serum samples of patients with CKD3-4, fetuin A was not associated with CV outcome, confirming earlier studies that this association is only observed in dialysis patients (*34*).

This study does have several limitations. Although circulating calprotectin showed an ability to predict CV outcome in both the CKD3-4 and the CKD5 Dialysis cohorts, this finding should be replicated in an independent validation cohort. Moreover, we did not investigate whether changes in circulating calprotectin in CKD could be associated with future CV events to assess the potential predictive value of an increase in calprotectin concentration. In the CKD5 cohort, calprotectin concentrations were associated with vascular calcification, but it should nevertheless be expected that the burden of CV disease in this selected group of patients, carefully evaluated for preemptive living-donor transplantation, could be less than in unselected patients with CKD5.

This study has identified calprotectin as a potential marker of and therapeutic target for CKD-associated calcification. We

believe that this study provides a comprehensive map of the CKD proteome associated with CVD and anticipate that it will serve as a reference for future studies to shed additional light on the pathophysiology of CV complications in patients with CKD.

MATERIALS AND METHODS

Study design

In this study, we aimed to determine the mechanisms of CV complications in CKD that may be used as starting points for therapeutic targets to protect against the development of vascular calcification. Identification of calprotectin was performed using untargeted mass spectrometry and ELISA in serum and plasma samples from three independent cohorts of patients with CKD. Functional studies were performed in vitro (primary hASMCs), ex vivo (mouse aortic rings), and in vivo in mouse models (subtotal nephrectomy mice and aged $ApoE^{-/-}$ mice). Information about the human participants is described in the "Study participants" section and detailed in Tables 1 to 3. All mouse studies were performed in accordance with National Institutes of Health guidelines and were approved by a local ethics committee. Randomization, blinding, and replication are specified in each applicable section. All sample sizes are indicated in the figure legends.

Study participants

For this study, we included participants with CKD stage 3 and 4, CKD stage 5 on hemodialysis, or CKD stage 5 from the following three cohorts (Tables 1 and 3).

CKD stage 3 and 4 (CKD3-4)

The NEFRONA study is a multicenter prospective cohort study of patients with CKD without a history of acute CV events at inclusion and with at least 4 years of follow-up (*13*). Patients were recruited from 81 primary care centers in Spain between October 2010 and June 2012. Patients aged 18 to 74 years were eligible if they had CKD stage 3 or higher as defined by current guidelines (eGFR < 60 ml/min per 1.73 m^2 estimated using the four-variable modification of diet in renal disease equation). Exclusion criteria were previous CV disease, active infections (HIV and tuberculosis), pregnancy, history of organ transplantation, and life expectancy of less than 1 year. Of the 2445 patients available in the NEFRONA study, we included 112 patients with CKD stage 3 or 4 (15 < eGFR < 60 ml/min per 1.73 m^2) and available serum samples. Demographic factors and relevant medical history were determined at patient recruitment using a detailed medical questionnaire. Biochemical parameters were obtained from a routine fasting blood test. The study protocol was approved by the local ethics committee of the Hospital Arnau de Vilanova, Lleida, Spain (review board number 13/2010) and conducted in accordance with the Declaration of Helsinki. All patients gave informed consent.

CKD stage 5 on hemodialysis (CKD5 Dialysis)

The CKDomic cohort recruited 171 patients on maintenance hemodialysis from the Toulouse University Hospital (Toulouse, France) and the AURAR-Dialysis center (La Reunion, France) and with a 2-year follow-up. Patients were included between June 2015 and January 2018. Patients underwent either hemodialysis or online hemodiafiltration. Demographic factors, relevant medical history, and medications were determined by medical record review. History of CV disease was defined as a history of myocardial infarction, unstable angina, stroke, and transient ischemic attack. Plasma samples were collected according to standardized procedures before dialysis, before anticoagulant administration. K-EDTA-plasma samples were processed immediately after collection and stored at −80°C. The study protocol was approved by the French ethics committee (review board number DC-2011-1388, CER 06-0115) and conducted in accordance with the Declaration of Helsinki. All patients gave informed consent.

CKD stage 5 (CKD5)

The Karolinska Hospital recruited patients (KärlTx cohort; 2008/748-31/2; 2019/01134) in the context of living-donor kidney transplantation by collecting clinical data, serum, and epigastric/iliac artery biopsies from kidney transplant recipients. This cohort enrolled, between March 2013 and May 2020, 255 clinically stable adults (age >18 years) with end-stage kidney failure (CKD stage 5) selected for kidney transplantation at the time of inclusion (*35*). Relevant demographics, comorbidities, medications, and routine biochemical parameters were extracted from electronic files. Biochemical parameters were obtained from a routine fasting blood test. CV disease was defined on the basis of clinical history or signs of ischemic cardiac disease, peripheral vascular disease, and/or cerebrovascular disease. During kidney transplantation surgery, a piece of the epigastric artery was harvested. Calcification was assessed histologically using Von Kossa staining. From this cohort, we included 170 patients with available serum samples, clinical data, and histological scoring of medial calcification. The study was conducted in adherence to the Declaration of Helsinki and approved by the ethical committees of Karolinska University Hospital. Written informed consent was obtained from each patient.

Outcomes of interest

Outcomes of interest during follow-up of the patients with CKD3-4 were fatal (n = 9) or nonfatal CV events (n = 30). CV mortality included death secondary to myocardial infarction, arrhythmia, congestive heart failure, stroke, aneurysm, mesenteric infarction, and sudden death. Nonfatal CV events included transient ischemic attack (n = 4), unstable angina (n = 11), stent (n = 4), myocardial infarction (n = 2), cerebrovascular accident (n = 4), and other CV event (n = 5). CV events were registered at each visit. For out-of-hospital deaths, family members were interviewed by telephone to better ascertain the circumstances of death. For patients with CKD5 on dialysis, the primary outcome was a composite outcome combining all-cause mortality (n = 24) and CV events (n = 18) including unstable angina, stent, myocardial infarction, and cerebrovascular accident. Information about all-cause mortality and CV events was classified on the basis of electronic medical records and reviewed by a physician.

Serum sample preparation for proteomic analysis

For proteomic analysis, we selected a case-control subset of 66 patients from the CKD stage 3 and 4 cohort: 32 cases and 34 matched controls. To reduce the dynamic range of protein concentrations, we used a strategy based on the combinatorial hexapeptide ligand library beads (ProteoMiner, Bio-Rad). About 10 mg of proteins (150-μl serum sample) diluted in 2 ml of phosphate-buffered saline (PBS) 1× was incubated with 20 μl of beads for 4 hours at room temperature on a rotor. Samples were then centrifuged. The beads were washed three times with wash buffer PBS 1× to remove unbound proteins. The proteins captured by the beads were eluted

by the addition of 15 μl of Laemmli sample buffer for electrophoresis. Then, protein concentration was measured using the Pierce BCA Protein Assay Kit (Thermo Fisher Scientific). Fifty micrograms of proteins was heated at 95°C for 5 min. Cysteines were alkylated using chloroacetamide (75 mM) for 30 min at room temperature. Proteins were loaded onto a 12% acrylamide SDS–polyacrylamide gel electrophoresis gel and concentrated in a single band visualized by Coomassie staining (Instant Blue, Expedeon). The gel band containing the whole sample was cut and washed several times in 50 mM ammonium bicarbonate:acetonitrile (1:1) for 15 min at 37°C. Proteins were in-gel-digested using 0.6 μg of modified sequencing-grade trypsin (Promega) in 50 mM ammonium bicarbonate overnight at 37°C. Peptides were extracted from the gel by two incubations in 10% formic acid:acetonitrile (1:1) for 15 min at 37°C. The extracted fractions were pooled with the initial digestion supernatant and dried under speed-vacuum. The resulting peptides were resuspended with 50 μl in 5% acetonitrile and 0.05% trifluoroacetic acid for nanoscale liquid chromatography–tandem mass spectrometry (nanoLC-MS/MS) analysis.

Proteomic analysis

Each sample (5 μl) was loaded onto a C18 precolumn [300 μm (inner diameter) × 5 mm; 5-μm particle size; 100-Å pore size; Dionex] at 20 μl/min in 5% acetonitrile and 0.05% trifluoroacetic acid. After 5 min of desalting, the precolumn was switched online with the analytical C18 column [75 μm (inner diameter) × 50 cm; 3-μm particle size; 120-Å pore size in house; packed with ReproSil C18] equilibrated in 95% solvent A (5% acetonitrile and 0.2% formic acid) and 5% solvent B (80% acetonitrile and 0.2% formic acid). Peptides were eluted using a 5 to 50% gradient of solvent B over 110 min at a flow rate of 300 nl/min. The mass spectrometer was operated in a data-dependent acquisition mode with Xcalibur software. Survey MS scans were acquired in the Orbitrap on the 300 to 2000 mass/charge ratio (m/z) range with the resolution set at 60,000. The 20 most intense ions per survey scan were selected for collision-induced dissociation (CID) fragmentation, and the resulting fragments were analyzed in the linear ion trap (LTQ). A dynamic exclusion of 60 s to prevent repetitive selection of the same peptide was applied.

Proteomic data processing

Raw nanoLC-MS/MS files were submitted to Mascot database searches (version 2.6.2, Matrix Science) against "Human" entries in the Swiss-Prot protein database (UniProtKB/Swiss-Prot protein knowledgebase release 2017_10; 20239 sequences entries). Carbamidomethylation of cysteine was set as a fixed modification, whereas oxidation of methionine and protein N-terminal acetylation were set as variable modifications. Specificity of trypsin digestion was set for cleavage after K or R, and two missed trypsin cleavage sites were allowed. The mass tolerance was set to 10 parts per million (ppm) for the precursor ion. It was set for fragment ions to 0.8 daltons in collision-induced dissociation (CID) mode and to 20 milli mass units in higher energy collisional dissociation (HCD) mode. Identification results were imported into Proline software (http://proline.profiproteomics.fr/) for validation. Peptide spectrum matches (PSM) with rank equal to one were retained. False discovery rate was then optimized to be below 1% at PSM level using Mascot-adjusted E value and below 1% at protein level using Mascot MudPIT score. For label-free quantification, peptide abundances were extracted using Proline software version 1.6 with an m/z tolerance set to 5 ppm. Alignment of LC-MS runs was performed using Loess smoothing. Cross-assignment of peptide ion abundances was performed among the samples using an m/z tolerance of 5 ppm and a retention time tolerance of 42 s. Protein abundances were computed using the median ratio fitting of the unique peptide abundances normalized at the peptide level. Only proteins that were quantified in at least 50% of the biological replicates in at least one of the groups were considered for further processing and statistical analysis. Remaining missing values were then replaced by a constant noise value determined independently for each analytical run as the 1% percentile of the total protein population.

Enrichment analysis

Gene enrichment and functional annotation analyses were performed using the DAVID tool (*36*, *37*). Term enrichment was considered for analysis when adjusted $P < 0.05$ and at least 10 proteins from the serum proteome analysis were annotated.

ELISA measurements

Serum and plasma calprotectin concentrations were determined in a blinded manner with commercially available ELISA kits for human (Bio-Techne, DS8900) or mice (Bio-Techne, DY8596-05) according to the manufacturer′s protocol. Plasma PTH (1-84) and FGF23 (C-term) concentrations were determined with commercially available mouse ELISA kits (Immutopics, #60-2305 and #60-6300, respectively) according to the manufacturer′s protocols.

Culture of primary hASMCs

Primary hASMCs (Lonza, CC-2571) were maintained at 37°C in a humidified atmosphere with 5% of CO_2 in SmGM BulletKit (Lonza, CC-3182) until confluence. For experiments, cells were split and cultivated in Dulbecco′s modified Eagle′s medium (DMEM) GlutaMAX supplemented with 2.5% of fetal bovine serum (FBS), penicillin (100 U/ml), and streptomycin (100 mg/ml). hASMCs from male and female donors (tissue acquisition nos. 26646, 25456, 35724, and 27930) were used in all experiments from passages 3 to 6 depending on the availability of the cells. All experiments were replicated in two to four independent cell passages, each with at least four biological replicates per group. To induce calcification, cells were treated with 2.6 mM NaH_2PO_4/25 mM Hepes for 3 days (ALPL activity) or 5 days (calcium measurement and alizarin red staining). Where indicated, hASMCs were prestimulated with paquinimod (10 μg/ml; DC Chemicals, DC10875), 3 μM TAK-242 (InvivoGen, CLI-095), or anti-RAGE antibody (10 μg/ml; R&D Systems, MAB11451) for 30 min followed by human recombinant calprotectin (10 μg/ml; Bio-Techne, 8226-S8-050). Equal amounts of vehicle or isotype immunoglobulin (R&D Systems, MAB004) were used as controls. Fresh media with agents were added every 2 to 3 days.

For experiments with human serum, 23 patients with CKD (13 male and 7 female) on dialysis and without diabetes were selected from the CKD5 (KärlTx) cohort and sex-matched with 16 healthy individuals (nine male and seven female) with normal renal function, without diabetes, CKD, or major illnesses from Ghent University Hospital (Belgium). Ethics approval was obtained by the local ethics committees at the Karolinska University Hospital (2008/748-31/2; 2019/01134) and the Ghent University Hospital (2010/033; B67020107926), and all participants gave informed consent, adhering to the Declaration of Helsinki. Primary female and male

hASMCs were cultivated with DMEM GlutaMAX and treated with 2.6 mM NaH_2PO_4/25 mM Hepes together with 15% of pooled female and male CKD/healthy serum, respectively, and paquinimod (10 μg/ml) or vehicle for 5 days. Detailed information about quantification of calcium deposition, alizarin red staining, and measurement of ALPL activity are provided in the Supplementary Materials.

Culture of mouse aortic rings

Abdominal aortas were dissected from 12-week-old male Swiss CD-1 mice (Janvier Labs). Connective tissue was gently removed, and aortas were cut in four or five rings of 2-mm length. Rings from one animal were randomly assigned to different treatment conditions. Rings were cultivated in DMEM supplemented with 2.5% of FBS, penicillin (100 U/ml), and streptomycin (100 mg/ml) at 37°C in a humidified atmosphere with 5% of CO_2. To induce calcification, aortic rings were stimulated with 1.8 mM NaH_2PO_4/25 mM Hepes for 7 days (calcium measurement and Von Kossa staining). Where indicated, aortic rings were prestimulated with paquinimod (10 μg/ml; DC Chemicals, DC10875) for 30 min followed by mouse recombinant calprotectin (10 μg/ml; R&D Systems, 8916-S8-050). Stimulation was performed every 2 days. Equal amounts of vehicle were used as controls. Fresh media with agents were added every 2 to 3 days. Detailed information about quantification of calcium deposition and Von Kossa staining are provided in the Supplementary Materials.

5/6 nephrectomy mouse model

Male and female DBA/2J mice (Charles River, France) were housed in a pathogen-free, temperature-controlled environment with a 12-hour light/12-hour dark cycle. Animals had free access to food and tap water. At reception, mice were randomly assigned in cages (four animals per cage), and cages were randomly assigned to four groups (n = 24 per group): (i) sham + vehicle, (ii) sham + paquinimod, (iii) subtotal nephrectomy (5/6 Nx) + vehicle, and (iv) 5/6 Nx + paquinimod. At 12 weeks of age, subtotal nephrectomy was performed using a two-step procedure (*38*). First, animals received subcutaneous injection of buprenorphine (Buprecare, 100 μg/kg) and were anesthetized with 2% isoflurane. The left kidney was exposed through midline abdominal incision. Upper and lower poles were resected and weighed. Two weeks later, the right kidney was exposed and removed through midline abdominal incision. In parallel, control animals underwent sham surgery (sham). After 1-week recovery, diet was switched to a phosphate-rich diet (C1031-modified 0.6% calcium and 0.9% phosphorus; Altromin), and mice were treated with paquinimod (5 μg/g per day, gavage) or vehicle 5 days a week for 8 weeks. Paquinimod (DC Chemicals, DC10875) was prepared at 0.75 mg/ml in 2.5% dimethyl sulfoxide, 10% polyethylene glycol, molecular weight 300, 1.25% Tween-80, and 86.25% saline solution. One group of 5/6 Nx mice did not receive the phosphate diet (normal diet). All animal experiments were performed in a nonblinded manner. Three animals died in the 5/6 Nx + vehicle group, and two died in the 5/6 Nx + paquinimod group. After 7 weeks, GFR was measured (n = 8 per group), and urine samples were collected in metabolic cages overnight (n = 14 per group). Urine samples were centrifuged for 5 min at 1500*g*, and supernatant was stored at −20°C. One urine sample in the sham + paquinimod group was excluded from analysis because it was contaminated with feces. After 8 weeks of treatment, mice were euthanized. Blood was harvested from the vena cava and collected in heparinized tubes (Microvette Hép-Lithium, Sarstedt) to avoid platelet aggregation. Blood was then centrifuged for 5 min at 1500*g*, and plasma was collected and immediately frozen at −80°C. All experiments were conducted in accordance with National Institutes of Health guidelines for the care and use of laboratory animals and were approved by a local ethics committee [Regional Centre for Functional Exploration and Experimental Resources (CREFRE)/US006 Inserm, Toulouse, France; #16445 2018082111041911]. Detailed information about GFR measurement, urine, and plasma biochemistry analysis and quantification of calcium deposition are provided in the Supplementary Materials.

Apolipoprotein E–deficient ($ApoE^{-/-}$) mouse model

Male and female $ApoE^{-/-}$ mice (Charles River, France) were housed in a pathogen-free, temperature-controlled environment with a 12-hour light/12-hour dark cycle. Animals had free access to food and tap water. Mice were housed in cages containing three or four animals, and cages were randomly assigned to two groups (n = 26 per group): (i) vehicle and (ii) paquinimod. At the age of 36 weeks (9 months), diet was switched to a phosphate-rich diet (C1031-modified 0.6% calcium and 0.9% phosphorus; Altromin), and mice were treated with paquinimod (5 μg/g per day, gavage) or vehicle 5 days a week for 8 weeks. All animal experiments were performed in a nonblinded manner. Three animals died in the vehicle group, and three died in the paquinimod group. Mice were euthanized at 44 weeks of age (11 months). Blood was harvested from the vena cava and collected in heparinized tubes (Microvette Hép-Lithium, Sarstedt) to avoid platelet aggregation. Blood was then centrifuged for 5 min at 1500*g*, and plasma was collected and immediately frozen at −80°C. All experiments were conducted in accordance with National Institutes of Health guidelines for the care and use of laboratory animals and were approved by a local ethics committee (Regional Centre for Functional Exploration and Experimental Resources (CREFRE)/US006 Inserm, Toulouse, France; #16445 2018082111041911). Detailed information about quantification of calcium deposition and histological staining are provided in the Supplementary Materials.

RNA extraction and reverse transcription quantitative polymerase chain reaction

Total RNA was isolated from thoracic aortic tissue using RNeasy Mini Kit (QIAGEN) according to the manufacturer's instructions. RNA concentration was measured with a NanoDrop spectrophotometer (Thermo Fisher Scientific), and samples with low RNA purity (260/230 ratio) were excluded from analysis. Reverse transcription of total RNA was performed using Maxima First Strand cDNA Synthesis (Thermo Fisher Scientific). Quantitative reverse transcription polymerase chain reaction (PCR) was performed with the ViiA 7 Real-Time PCR System (Applied Biosystems) and Perfecta SYBR Green SuperMix (Quanta bio) according to the manufacturer's instructions. All PCRs were performed in duplicate, and relative mRNA expression was calculated by the $2^{-\Delta\Delta Ct}$ method, using *GAPDH* as housekeeping gene normalized to the control group. The following mouse primers were used: *Runx2* forward, 5′ AGA GTC AGA TTA CAG ATC CCA GG 3′; *Runx2* reverse, 5′ AGG AGG GGT AAG ACT GGT CAT A 3′; *Msx2* forward, 5′ TTC ACC ACA TCC CAG CTT CTA 3′; *Msx2* reverse, 5′ TTG CAG TCT TTT CGC CTT AGC 3′; *GAPDH* forward, 5′ AGG TCG GTG TGA

ACG GAT TTG 3′; and *GAPDH* reverse:, 5′ TGT AGA CCA TGT AGT TGA GGT CA 3′.

Statistical analyses

Serum proteome abundances were log-transformed, whereas other variables were not transformed. In the 112 patients of the CKD3-4 cohort, the number of missing values ranged from 0 to 3 for each clinical parameter, except for PTH (22 missing values), low-density lipoprotein (LDL) cholesterol (10 missing values), and high-density lipoprotein (HDL) cholesterol (10 missing values). In the 171 patients of the CKD5 Dialysis cohort, the number of missing values ranged from 0 to 4 for each clinical parameter, except for PTH (79 missing values), LDL cholesterol (79 missing values), HDL cholesterol (79 missing values), and smoking status (27 missing values). Missing values were handled using the available case approach (pairwise deletion), meaning that missing values were ignored when analyzing the respective variable. Spearman rank correlation was used to determine correlations between variables. For proteome data, *P* values were adjusted for multiple testing using the Benjamini-Hochberg procedure. Multivariate feature ranking of the most prominent serum proteome changes was based on importance measurement (mean decrease in accuracy) extracted from a tuned RF model [tunegrid-based mtry optimization using repeated cross-validation on accuracy metric, ntree optimization to stabilize out-of-bag (OOB) error rate; final tuning: mtry = 10, ntree = 2000, OOB rate = 1.5%]. Univariate and multivariate linear regression analyses were applied to quantify the association of circulating calprotectin with clinically relevant variables at baseline, including age, sex, body mass index, CRP, eGFR (for CKD3-4) or time on dialysis (for CKD5 Dialysis), albumin, Ca × P product, dyslipidemia, diabetes, and hypertension. Analysis of covariance (ANCOVA) using CRP or age (per 10 years), male sex, and diabetes as covariates was used to assess the differences between groups for calprotectin. Survival analyses were displayed using Kaplan-Meier curves and compared using log-rank test. Patients were censored as free of outcome when they reached the planned end of study without experiencing the outcome of interest or were lost to follow-up. Univariate and multivariate Cox proportional hazard models were built to estimate impact of baseline parameters on survival. Proportional hazard hypothesis and model′s performance using Harrell′s C index were verified for every model. Results were presented as hazard ratio and 95% CIs. To study the ability of baseline parameters to predict CV outcome, conventional CV RFs were combined with or without calprotectin using a logistic regression model. Performances were assessed by calculating the AUC and 95% CI (DeLong method). Comparisons between model performances were done using the DeLong test. Data normality was analyzed using the Shapiro-Wilk normality test. For normally distributed data, statistical analysis was performed with two-sided Student′s *t* test for comparison between two groups, one-way analysis of variance (ANOVA) test followed by Šidák′s multiple comparisons, and two-way ANOVA test followed by Tukey′s multiple comparisons for effects of two variables. The Mann-Whitney *U* test or Kruskal-Wallis test with Dunn′s multiple comparisons were used for non-normally distributed data. For categorical variables, Fisher′s exact test or the chi-square test was used as appropriate. Outliers were detected using the robust regression and outlier removal method and excluded from analysis. A $P < 0.05$ was considered as significant.

Supplementary Materials

This PDF file includes:
Materials and Methods
Figs. S1 to S3
Tables S1 to S7
STROBE Checklist

Other Supplementary Material for this manuscript includes the following:
Data file S1
MDAR Reproducibility Checklist

REFERENCES AND NOTES

1. GBD Chronic Kidney Disease Collaboration, Global, regional, and national burden of chronic kidney disease, 1990–2017: A systematic analysis for the Global Burden of Disease Study 2017. *Lancet* **395**, 709–733 (2020).
2. A. Ortiz, A. Covic, D. Fliser, D. Fouque, D. Goldsmith, M. Kanbay, F. Mallamaci, Z. A. Massy, P. Rossignol, R. Vanholder, A. Wiecek, C. Zoccali, G. M. London; Board of the EURECA-m Working Group of ERA-EDTA, Epidemiology, contributors to, and clinical trials of mortality risk in chronic kidney failure. *Lancet* **383**, 1831–1843 (2014).
3. M. Cano-Megías, P. Guisado-Vasco, H. Bouarich, G. de Arriba-de la Fuente, P. de Sequera-Ortiz, C. Álvarez-Sanz, D. Rodríguez-Puyol, Coronary calcification as a predictor of cardiovascular mortality in advanced chronic kidney disease: A prospective long-term follow-up study. *BMC Nephrol.* **20**, 188 (2019).
4. A. Y.-M. Wang, M. Wang, J. Woo, C. W.-K. Lam, P. K.-T. Li, S.-F. Lui, J. E. Sanderson, Cardiac valve calcification as an important predictor for all-cause mortality and cardiovascular mortality in long-term peritoneal dialysis patients: A prospective study. *J. Am. Soc. Nephrol.* **14**, 159–168 (2003).
5. J. Voelkl, F. Lang, K.-U. Eckardt, K. Amann, M. Kuro-O, A. Pasch, B. Pieske, I. Alesutan, Signaling pathways involved in vascular smooth muscle cell calcification during hyperphosphatemia. *Cell. Mol. Life Sci.* **76**, 2077–2091 (2019).
6. A. L. Durham, M. Y. Speer, M. Scatena, C. M. Giachelli, C. M. Shanahan, Role of smooth muscle cells in vascular calcification: Implications in atherosclerosis and arterial stiffness. *Cardiovasc. Res.* **114**, 590–600 (2018).
7. W. C. O'Neill, K. A. Lomashvili, Recent progress in the treatment of vascular calcification. *Kidney Int.* **78**, 1232–1239 (2010).
8. G. Glorieux, W. Mullen, F. Duranton, S. Filip, N. Gayrard, H. Husi, E. Schepers, N. Neirynck, J. P. Schanstra, J. Jankowski, H. Mischak, À. Argilés, R. Vanholder, A. Vlahou, J. Klein, New insights in molecular mechanisms involved in chronic kidney disease using high-resolution plasma proteome analysis. *Nephrol. Dial. Transplant.* **30**, 1842–1852 (2015).
9. T. Feldreich, C. Nowak, A. C. Carlsson, C.-J. Östgren, F. H. Nyström, J. Sundström, J.-J. Carrero-Roig, J. Leppert, P. Hedberg, V. Giedraitis, L. Lind, A. Cordeiro, J. Ärnlöv, The association between plasma proteomics and incident cardiovascular disease identifies MMP-12 as a promising cardiovascular risk marker in patients with chronic kidney disease. *Atherosclerosis* **307**, 11–15 (2020).
10. M. Luczak, D. Formanowicz, Ł. Marczak, J. Suszyńska-Zajczyk, E. Pawliczak, M. Wanic-Kossowska, M. Stobiecki, iTRAQ-based proteomic analysis of plasma reveals abnormalities in lipid metabolism proteins in chronic kidney disease-related atherosclerosis. *Sci. Rep.* **6**, 32511 (2016).
11. I. Ruderman, S. G. Holt, T. D. Hewitson, E. R. Smith, N. D. Toussaint, Current and potential therapeutic strategies for the management of vascular calcification in patients with chronic kidney disease including those on dialysis. *Semin. Dial.* **31**, 487–499 (2018).
12. P. Raggi, A. Bellasi, D. Bushinsky, J. Bover, M. Rodriguez, M. Ketteler, S. Sinha, C. Salcedo, K. Gillotti, C. Padgett, R. Garg, A. Gold, J. Perelló, G. M. Chertow, Slowing progression of cardiovascular calcification with SNF472 in patients on hemodialysis. *Circulation* **141**, 728–739 (2020).
13. M. Junyent, M. Martínez, M. Borràs, B. Coll, J. M. Valdivielso, T. Vidal, F. Sarró, J. Roig, L. Craver, E. Fernández, Predicting cardiovascular disease morbidity and mortality in chronic kidney disease in Spain. The rationale and design of NEFRONA: A prospective, multicenter, observational cohort study. *BMC Nephrol.* **11**, 14 (2010).
14. S. Wang, R. Song, Z. Wang, Z. Jing, S. Wang, J. Ma, S100A8/A9 in inflammation. *Front. Immunol.* **9**, 1298 (2018).
15. M. Pruenster, T. Vogl, J. Roth, M. Sperandio, S100A8/A9: From basic science to clinical application. *Pharmacol. Ther.* **167**, 120–131 (2016).
16. A. Silvin, N. Chapuis, G. Dunsmore, A.-G. Goubet, A. Dubuisson, L. Derosa, C. Almire, C. Hénon, O. Kosmider, N. Droin, P. Rameau, C. Catelain, A. Alfaro, C. Dussiau, C. Friedrich, E. Sourdeau, N. Marin, T.-A. Szwebel, D. Cantin, L. Mouthon, D. Borderie, M. Deloger, D. Bredel, S. Mouraud, D. Drubay, M. Andrieu, A.-S. Lhonneur, V. Saada, A. Stoclin, C. Willekens, F.

Pommeret, F. Griscelli, L. G. Ng, Z. Zhang, P. Bost, I. Amit, F. Barlesi, A. Marabelle, F. Pène, B. Gachot, F. André, L. Zitvogel, F. Ginhoux, M. Fontenay, E. Solary, Elevated calprotectin and abnormal myeloid cell subsets discriminate severe from mild COVID-19. *Cell* **182**, 1401–1418.e18 (2020).

17. K. Malícková, H. Brodská, J. Lachmanová, S. Dusilová Sulková, I. Janatková, H. Marecková, V. Tesar, T. Zima, Plasma calprotectin in chronically dialyzed end-stage renal disease patients. *Inflamm. Res.* **59**, 299–305 (2010).
18. S. Bieber, K. A. Muczynski, C. Lood, Neutrophil activation and neutrophil extracellular trap formation in dialysis patients. *Kidney Med.* **2**, 692–698.e1 (2020).
19. T. Kanki, T. Kuwabara, J. Morinaga, H. Fukami, S. Umemoto, D. Fujimoto, T. Mizumoto, M. Hayata, Y. Kakizoe, Y. Izumi, S. Tajiri, T. Tajiri, K. Kitamura, M. Mukoyama, The predictive role of serum calprotectin on mortality in hemodialysis patients with high phosphoremia. *BMC Nephrol.* **21**, 158 (2020).
20. P. Y.-K. Poon, C.-C. Szeto, B. C.-H. Kwan, K.-M. Chow, C.-B. Leung, P. K.-T. Li, Relationship between myeloid-related protein 8/14 and survival of Chinese peritoneal dialysis patients. *Kidney Blood Press. Res.* **35**, 489–496 (2012).
21. M. Montagnana, E. Danese, G. Lippi, Calprotectin and cardiovascular events. A narrative review. *Clin. Biochem.* **47**, 996–1001 (2014).
22. J. Marta-Enguita, M. Navarro-Oviedo, I. Rubio-Baines, N. Aymerich, M. Herrera, B. Zandio, S. Mayor, J.-A. Rodriguez, J.-A. Páramo, E. Toledo, M. Mendioroz, R. Muñoz, J. Orbe, Association of calprotectin with other inflammatory parameters in the prediction of mortality for ischemic stroke. *J. Neuroinflammation* **18**, 3 (2021).
23. S. K. Kunutsor, J. L. Flores-Guerrero, L. M. Kieneker, T. Nilsen, C. Hidden, E. Sundrehagen, S. Seidu, R. P. F. Dullaart, S. J. L. Bakker, Plasma calprotectin and risk of cardiovascular disease: Findings from the PREVEND prospective cohort study. *Atherosclerosis* **275**, 205–213 (2018).
24. L. Pedersen, M. Nybo, M. K. Poulsen, J. E. Henriksen, J. Dahl, L. M. Rasmussen, Plasma calprotectin and its association with cardiovascular disease manifestations, obesity and the metabolic syndrome in type 2 diabetes mellitus patients. *BMC Cardiovasc. Disord.* **14**, 196 (2014).
25. D. Zhang, X. Bi, Y. Liu, Y. Huang, J. Xiong, X. Xu, T. Xiao, Y. Yu, W. Jiang, Y. Huang, J. Zhang, B. Zhang, J. Zhao, High phosphate-induced calcification of vascular smooth muscle cells is associated with the TLR4/NF-κb signaling pathway. *Kidney Blood Press. Res.* **42**, 1205–1215 (2017).
26. E. Simard, T. Söllradl, J.-S. Maltais, J. Boucher, P. D'Orléans-Juste, M. Grandbois, Receptor for advanced glycation end-products signaling interferes with the vascular smooth muscle cell contractile phenotype and function. *PLOS ONE* **10**, e0128881 (2015).
27. R. Kawakami, S. Katsuki, R. Travers, D. C. Romero, D. Becker-Greene, L. S. A. Passos, H. Higashi, M. C. Blaser, G. K. Sukhova, J. Buttigieg, D. Kopriva, A. M. Schmidt, D. G. Anderson, S. A. Singh, L. Cardoso, S. Weinbaum, P. Libby, M. Aikawa, K. Croce, E. Aikawa, S100A9-RAGE axis accelerates formation of macrophage-mediated extracellular vesicle microcalcification in diabetes mellitus. *Arterioscler. Thromb. Vasc. Biol.* **40**, 1838–1853 (2020).
28. R. Pecoits-Filho, B. Lindholm, P. Stenvinkel, The malnutrition, inflammation, and atherosclerosis (MIA) syndrome—The heart of the matter. *Nephrol. Dial. Transplant.* **17**, 28–31 (2002).
29. F. Boros, L. Vécsei, Progress in the development of kynurenine and quinoline-3-carboxamide-derived drugs. *Expert Opin. Investig. Drugs* **29**, 1223–1247 (2020).
30. M. Zahran, F. M. Nasr, A. A. Metwaly, N. El-Sheikh, N. S. A. Khalil, T. Harba, The role of hemostatic factors in atherosclerosis in patients with chronic renal disease. *Electron. Physician* **7**, 1270–1276 (2015).
31. S. H. Baek, R.-H. Cha, S. W. Kang, C. W. Park, D. R. Cha, S. G. Kim, S. A. Yoon, S. Kim, S. Y. Han, J. H. Park, J. H. Chang, C. S. Lim, Y. S. Kim, K. Y. Na, Higher serum levels of osteoglycin are associated with all-cause mortality and cardiovascular and cerebrovascular events in patients with advanced chronic kidney disease. *Tohoku J. Exp. Med.* **242**, 281–290 (2017).
32. N. Ozkayar, S. Piskinpasa, F. Akyel, D. Turgut, M. Bulut, T. Turhan, F. Dede, Relation between serum cathepsin D levels and endothelial dysfunction in patients with chronic kidney disease. *Nefrología* **35**, 72–79 (2015).
33. A. L. Durham, M. Y. Speer, M. Scatena, C. M. Giachelli, C. M. Shanahan, Role of smooth muscle cells in vascular calcification: Implications in atherosclerosis and arterial stiffness. *Cardiovasc. Res.* **114**, 590–600 (2018).
34. Z. Zhou, Y. Ji, H. Ju, H. Chen, M. Sun, Circulating fetuin-A and risk of all-cause mortality in patients with chronic kidney disease: A systematic review and meta-analysis. *Front. Physiol.* **10**, (2019).
35. L. Dai, L. Li, H. Erlandsson, A. M. G. Jaminon, A. R. Qureshi, J. Ripsweden, T. B. Brismar, A. Witasp, O. Heimbürger, H. S. Jørgensen, P. Barany, B. Lindholm, P. Evenepoel, L. J. Schurgers, P. Stenvinkel, Functional vitamin K insufficiency, vascular calcification and mortality in advanced chronic kidney disease: A cohort study. *PLOS ONE* **16**, e0247623 (2021).
36. D. W. Huang, B. T. Sherman, R. A. Lempicki, Bioinformatics enrichment tools: Paths toward the comprehensive functional analysis of large gene lists. *Nucleic Acids Res.* **37**, 1–13 (2009).
37. D. W. Huang, B. T. Sherman, R. A. Lempicki, Systematic and integrative analysis of large gene lists using DAVID bioinformatics resources. *Nat. Protoc.* **4**, 44–57 (2009).
38. J. Voelkl, T. T. D. Luong, R. Tuffaha, K. Musculus, T. Auer, X. Lian, C. Daniel, D. Zickler, B. Boehme, M. Sacherer, B. Metzler, D. Kuhl, M. Gollasch, K. Amann, D. N. Müller, B. Pieske, F. Lang, I. Alesutan, SGK1 induces vascular smooth muscle cell calcification through NF-κB signaling. *J. Clin. Invest.* **128**, 3024–3040 (2018).

Acknowledgments: We would like to express our gratitude to all the nursing and medical staff from the hospitals and dialysis centers who participated and helped in the realization of this study. We thank the Phenotyping Department of the UMS006 CREFRE-Anexplo Platform and the GeT-Santé facility (I2MC, Inserm, Génome et Transcriptome, GenoToul, Toulouse, France) for technical support. G.G., P.S., and J.P.S. are members of the European Toxin Working Group. **Funding:** This work was supported by the European Union's Horizon 2020 research and innovation program under the Marie Skłodowska-Curie Caresyan, grant agreement no. 764474 to A.A.-G., J.K., J.P.S., K.K., P.S., and S.H.; European Union ERA CVD JTC2017, PROACT, grant number ANR-17-ECVD-0006 to J.-S.S.-B. and J.P.S.; University Hospital Toulouse, local grant 2016, no. RC31/16-8250 to A.A.-G., J.K., and S.F.; "Fondation pour la Recherche Médicale," grant no. DEQ20170336759 to J.K. and J.P.S.; "Société Francophone de Néphrologie, Dialyse et Transplantation" to A.A.-G. and J.K.; National Research Agency, Calprotect grant no. ANR-21-CE14-0013-01 to A.A.-G., J.K., and M. Brunet.; AURAR to J.-L.B. and S. Ardeleanu; French Ministry of Research with the Investissement d'Avenir Infrastructures Nationales en Biologie et Santé program (PIA, Proteomics French Infrastructure project), grant ProFI, ANR-10-INBS-08 to O.B.-S.; Instituto de Salud Carlos III and FEDER funds, grants PI18/00610 and RETIC RD16/0009 to J.M.V.; Ministerio de Ciencia, Innovación y Universidades, grant IJC2018-037792-I to J.M.V.; FEDER-région Occitanie, Program INSPIRE to J.K. and J.P.S.; Heart and Lung Foundation to P.S.; and Kidney Foundation and Research Council, Vetenskapsrådet 2018-00932 to P.S. **Author contributions:** Conceptualization: J.-L.B., J.K., J.M.V., J.P.S., K.K., and P.S. Methodology: A.A.-G., A.P., J.K., J.V., M.B., and M.C. Investigation: A.A.-G., A.C., A.D.B., A.P., A.R., B.B., B.B.-M., C.D., C.F., E.A., E.N., G.F., G.G., I.F., J.-L.B., J.M., J.M.V., J.-S.S.-B., L.G., M.A., M. Brunet, M. Buléon, M.B.-L., M.C., O.B.-S., S. Ardeleanu, S. Arefin, S.F., and S.H. Supervision: J.K., K.K., and P.S. Writing (original draft): A.A.-G., A.P., J.K., and J.P.S. Writing (review and editing): all co-authors. **Competing interests:** S.F. declares consulting fees from Abionyx Pharma, Novartis SA, Sanofi-Genzyme, CSL-Vifor, and Alexion and symposium and congress invitations from CSL-Vifor and Alexion. A.D.B. declares participation to speakers bureau and lectures for Hansa Pharma, Chiesi Pharma, Astellas, and Neovii. P.S. has been on scientific advisory boards (unrelated to the study) for FMC, Baxter, GSK, Astra Zeneca, CSL, Behring, Vifor, Reata, and Invizius. P.S. has also given lectures (unrelated to the study) at events sponsored by FMC, Baxter, Pfizer, Astra Zeneca, Astellas, Novi Nordisk, and Bayer. The other authors declare that they have no competing interests. **Data and materials availability:** All data associated with this study are present in the paper or the Supplementary Materials. The mass spectrometry proteomics data have been deposited to the ProteomeXchange Consortium via the PRIDE partner repository with the dataset identifier PXD024553. Serum samples from the 16 controls are available from G.G. under a material transfer agreement with Ghent University Hospital.

Submitted 7 December 2021
Accepted 17 August 2023
Published 6 September 2023
10.1126/scitranslmed.abn5939

Science Translational Medicine

Calprotectin is a contributor to and potential therapeutic target for vascular calcification in chronic kidney disease

Ana Amaya-Garrido, Manon Brunet, Bénédicte Buffin-Meyer, Alexis Piedrafita, Lucile Grzesiak, Ezechiel Agbegbo, Arnaud Del Bello, Inés Ferrandiz, Serban Ardeleanu, Marcelino Bermudez-Lopez, Camille Fedou, Mylène Camus, Odile Burlet-Schiltz, Jean Massines, Marie Buléon, Guylène Feuillet, Melinda Alves, Eric Neau, Audrey Casemayou, Benjamin Breuil, Jean-Sébastien Saulnier-Blache, Colette Denis, Jakob Voelkl, Griet Glorieux, Sam Hobson, Samsul Arefin, Awahan Rahman, Karolina Kublickiene, Peter Stenvinkel, Jean-Loup Bascands, Stanislas Faguer, José M. Valdivielso, Joost P. Schanstra, and Julie Klein

Sci. Transl. Med., **15** (712), eabn5939.
DOI: 10.1126/scitranslmed.abn5939